Journal of Geophysical Research: Atmospheres

RESEARCH ARTICLE

Key Points:
- Physical driving factors govern the concentration of PM$_{2.5}$
- Morning and evening rush hours coincide with enhanced levels of CO and NO$_2$
- EC is associated with biomass burning, while OC is mainly due to secondary sources

Comprehensive assessment of PM$_{2.5}$ physicochemical properties during the Southeast Asia dry season (southwest monsoon)

Md Firoz Khan[1] , Nor Azura Sulong[2], Mohd Talib Latif[2,3], Mohd Shahrul Mohd Nadzir[1,2], Norhaniza Amil[4], Dini Fajrina Mohd Hussain[2], Vernon Lee[2], Puteri Nurafidah Hosaini[2], Suhana Shaharom[2], Nur Amira Yasmin Mohd Yusoff[2], Hossain Mohammed Syedul Hoque[2], Jing Xiang Chung[2] , Mazrura Sahani[5], Norhayati Mohd Tahir[6,7], Liew Juneng[2], Khairul Nizam Abdul Maulud[8,9], Sharifah Mastura Syed Abdullah[10,11], Yusuke Fujii[12], Susumu Tohno[13], and Akira Mizohata[14]

[1]Centre for Tropical Climate Change System, Institute of Climate Change, Universiti Kebangsaan Malaysia, Bangi, Malaysia, [2]School of Environmental and Natural Resource Sciences, Faculty of Science and Technology, Universiti Kebangsaan Malaysia, Bangi, Malaysia, [3]Institute for Environment and Development (Lestari), Universiti Kebangsaan Malaysia, Bangi, Malaysia, [4]Environmental Technology Division, School of Industrial Technology, Universiti Sains Malaysia, Minden, Malaysia, [5]Environmental Health and Industrial Safety Program, School of Diagnostics and Applied Health Sciences, Faculty of Health Sciences, Universiti Kebangsaan Malaysia, Kuala Lumpur, Malaysia, [6]Environmental Research Group, School of Marine and Environment Sciences, Universiti Malaysia Terengganu, Kuala Terengganu, Malaysia, [7]Institute of Oceanography, Universiti Malaysia Terengganu, Kuala Terengganu, Malaysia, [8]Earth Observation Centre, Institute of Climate Change, Universiti Kebangsaan Malaysia, Bangi, Malaysia, [9]Department of Civil and Structural Department, Faculty of Engineering and Built Environment, Universiti Kebangsaan Malaysia, Bangi, Malaysia, [10]School of Social, Development and Environmental Studies, Faculty of Social Sciences and Humanities, Universiti, Kebangsaan, Bangi, Malaysia, [11]Institute of Climate Change, Universiti Kebangsaan Malaysia, Bangi, Malaysia, [12]Centre for Environmental Sciences in Saitama, Saitama, Japan, [13]Department of Socio-Environmental Energy Science, Graduate School of Energy Science, Kyoto University, Kyoto, Japan, [14]Research Organization for University-Community Collaborations, Osaka Prefecture University, Osaka, Japan

Abstract A comprehensive assessment of fine particulate matter (PM$_{2.5}$) compositions during the Southeast Asia dry season is presented. Samples of PM$_{2.5}$ were collected between 24 June and 14 September 2014 using a high-volume sampler. Water-soluble ions, trace species, rare earth elements, and a range of elemental carbon (EC) and organic carbon were analyzed. The characterization and source apportionment of PM$_{2.5}$ were investigated. The results showed that the 24 h PM$_{2.5}$ concentration ranged from 6.64 to 68.2 $\mu g\,m^{-3}$. Meteorological driving factors strongly governed the diurnal concentration of aerosol, while the traffic in the morning and evening rush hours coincided with higher levels of CO and NO$_2$. The correlation analysis for non sea-salt K$^+$-EC showed that EC is potentially associated with biomass burning events, while the formation of secondary organic carbon had a moderate association with motor vehicle emissions. Positive matrix factorization (PMF) version 5.0 identified the sources of PM$_{2.5}$: (i) biomass burning coupled with sea salt [I] (7%), (ii) aged sea salt and mixed industrial emissions (5%), (iii) road dust and fuel oil combustion (7%), (iv) coal-fired combustion (25%), (v) mineral dust (8%), (vi) secondary inorganic aerosol (SIA) coupled with F$^-$ (15%), and (vii) motor vehicle emissions coupled with sea salt [II] (24%). Motor vehicle emissions, SIA, and coal-fired power plant are the predominant sources contributing to PM$_{2.5}$. The response of the potential source contribution function and Hybrid Single-Particle Lagrangian Integrated Trajectory backward trajectory model suggest that the outline of source regions were consistent to the sources by PMF 5.0.

1. Introduction

Widespread transboundary polluted air is one of the main concerns for those living in Southeast Asia (SEA). Atmospheric particles have a damaging effect on human health. The World Health Organization (WHO) reported the death of approximately 3.7 million people worldwide in 2012 due to outdoor urban and rural sources of air pollution. In the western Pacific and SEA alone, the reported number of deaths due to emissions from heavy industry was cited at about 2.6 million, and this region was noted to contain the largest count of air pollution hotspots in 2012 [*World Health Organization*, 2014]. PM$_{2.5}$ (particles with an aerodynamic diameter of less than or equal to 2.5 μm) has a damaging effect on human health due to its ability to

penetrate deep into the lungs. *Pope et al.* [2009] reported that the reduction in $PM_{2.5}$ concentrations between the years 1980 and 2000 was strongly associated with a 2.7 year overall increase in life expectancy, which occurred during the same period, using data from 51 cities in the U.S. Furthermore, it is estimated that a $10 \, \mu g \, m^{-3}$ reduction in the annual average $PM_{2.5}$ would have a much larger impact on life expectancy in England and Wales than the complete elimination of road traffic accidents or passive smoking [*Institute of Occupational Medicine*, 2006]. *Heil and Goldammer* [2001] identified that the atmospheric particle loading during the smoke-haze episode was predominantly impacted due to an increase of the $PM_{2.5}$. In Malaysia, the smoke haze impacts severely on the human health and economy. A study by *Othman et al.* [2014] observed an association of smoke haze to an increase in inpatient cases by 2.4 per 10,000 people each year, representing an increase of 31% from non-haze days. The average annual economic loss due to the inpatient health impact of haze was valued at MYR273,000 ($91,000 USD) in Malaysia.

Aerosol particles, primarily originating from biomass burning and the combustion of peat soil, are strongly influenced by low-level monsoon circulation. Flame and smoldering combustion often occur in high-biomass and peatland areas, which have become major annual sources of aerosol, and other pollutants such as trace gases in SEA countries [*Levine*, 1999; *Stockwell et al.*, 2016; *Yokelson et al.*, 1997]. In SEA, the common practice of burning agricultural residues enhances haze pollution. "Slash and burn" is a common practice as it is the most cost efficient method in the management of agricultural waste and the clearing of land for cultivation [*Page et al.*, 2002]. There are widespread misconceptions and knowledge gaps regarding transboundary haze pollution and the chemical signatures of surface level fires and peatland burning occurring in SEA. An observation modeled by *Heil et al.* [2007] showed that when considering peat fires in an emission inventory, ambient particle concentrations exceed the ambient air quality standard across transboundary scales. However, when considering surface vegetation fires, ambient air quality standards are exceeded only in areas close to the main fires. Monsoon circulations and local wind systems are two further driving factors, which greatly influence the transport of aerosol pollution in this region [*Khan et al.*, 2016a; *Juneng et al.*, 2011; *Latif et al.*, 2014]. Together with slash and burn, wildfires, and peatland burning, combustion from the consumption of fossil fuels and vehicle emissions, industrial emissions, and quasi-open burning can also contribute to and produce a high amount of aerosol particles that influence the formation of haze [*Keywood et al.*, 2003]. In addition, Malaysia is a rapidly developing country in SEA that aims to achieve high-income country status by 2020; its economic growth is highly dependent on its abundant energy resources, especially natural gas and crude oil. Malaysia's energy use depends heavily on fossil fuels, including oil, gas, and coal. The energy consumption of the end-use sector in 2011 was 1.9 million tons of oil equivalent (Mtoe) for hydropower, 14.8 Mtoe for coal, 17.5 Mtoe for natural gas, 19.7 Mtoe vehicle fuel, and 8.9 Mtoe for crude oil [*Chong et al.*, 2015]. The energy consumption directly affects the level of air pollution and thus showed a linear positive correlation [*Khan et al.*, 2016b].

The source apportionment (SA) of aerosol particles is a widely applied method used to study the source of pollutants in the atmosphere. As an apportionment tool, multivariate receptor models can predict information regarding the sources of air pollutants. The output of a receptor model identifies the pollution source types. Additionally, it estimates the contribution of the identified sources to the observed concentration. Models presume the contribution of pollutant sources by determining the best fit linear combination for the emission source [*Schauer et al.*, 1996]. The most widely used models are chemical mass balance models [*Watson et al.*, 1990] and positive matrix factorization (PMF) [*Paatero and Tapper*, 1994], while the less popular models include UNMIX [*Henry*, 1987], a receptor model that can estimate the number of sources, source compositions, and source contributions to each sample, and principal component analysis coupled with absolute principal component score (PCA/APCS) [*Thurston and Spengler*, 1985]. PMF is the most preferred and robust model. PMF uses an implicit least squares fit which minimizes the sum of the square of the residuals. According to *Paatero and Tapper* [1994], the scaling of data by column and row leads to a distortion of the analysis. However, the factor-based models use an eigenvector analysis based on the decomposition of a singular value. The weights are based on known standard deviations in the species of the data matrix [*Hopke*, 2003; *Paatero*, 1997]. The advantage of the PMF model is the inclusion of uncertainties for each variable, which ensures that variables with large uncertainties have less influence on the output results. Numerous studies have been conducted using the PMF receptor model [*Amil et al.*, 2016; *Harrison et al.*, 2011; *Hasheminassab et al.*, 2014; *Khan et al.*, 2012; *Khan et al.*, 2015c; *Khan et al.*, 2016a; *Lestari and Mauliadi*, 2009; *Yu et al.*, 2013; *Zhang et al.*, 2013]. *Khan et al.* [2016a] discussed in detail the advantage of the
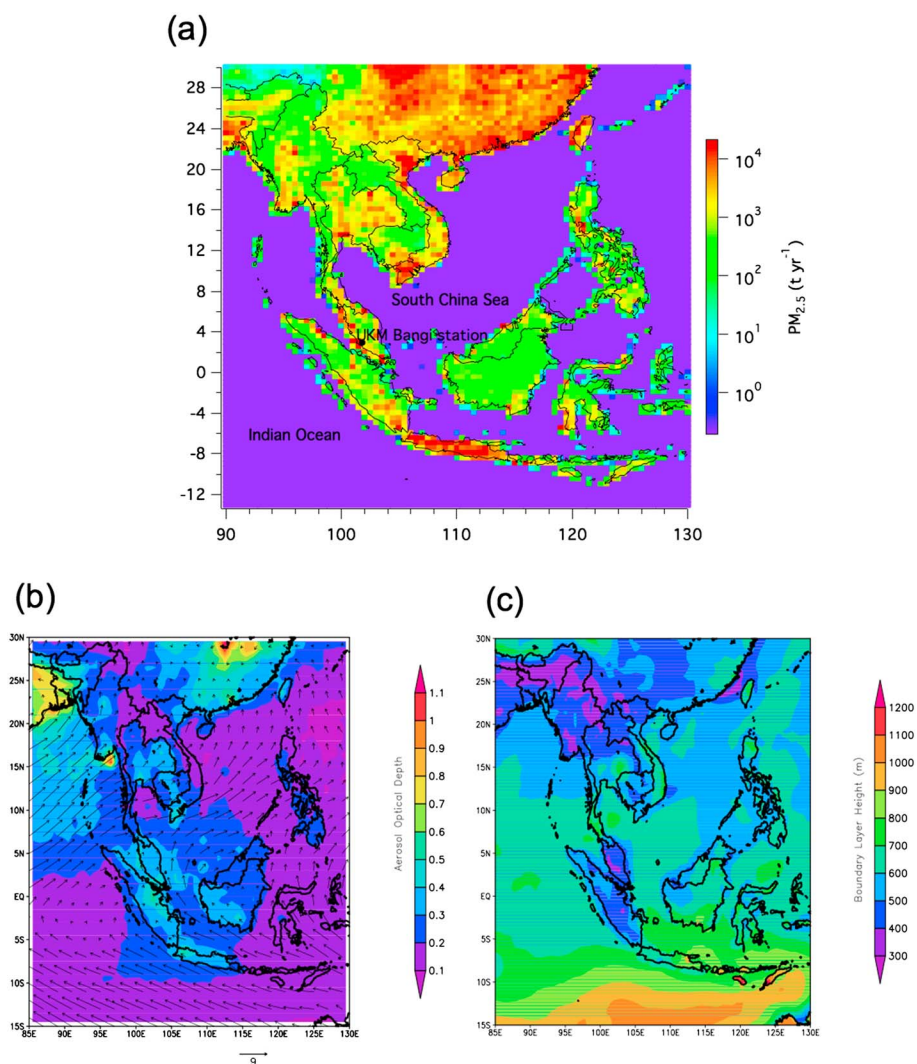
Figure 1. Location of the sampling site annotated to (a) the distribution of anthropogenic emission map (30×30 min resolution) in SEA in 2006 (data source: *Zhang et al.* [2009]), (b) spatial distribution of aerosol optical depth retrieved from Moderate Resolution Imaging Spectroradiometer (MODIS) Aqua and Terra level 3 data coupled with synoptic circulation of wind vector, and (c) the spatial variation of boundary layer height or mixing depth (m).

application of receptor models with a provision on how to generate robust results with minimum uncertainty. *Jamhari et al.* [2014] and *Mustaffa et al.* [2014] applied PCA/APCS to identify the sources of organic and inorganic compositions in airborne particulate matter in Malaysia. *Khan et al.* [2015c] have successfully introduced PMF version 5.0, an advanced and modified receptor tool in Malaysia using organic compositions of $PM_{2.5}$ in the Bangi area. In 2016, the sources of $PM_{2.5}$, based on the detailed inorganic compositions, were brought to light with the application of PMF 5.0 by *Amil et al.* [2016] and *Khan et al.* [2016a]. A similar approach was successfully applied in other Southeast Asian countries. For example, *Lestari and Mauliadi* [2009] and *Santoso et al.* [2008] used PMF to determine the sources of particulate matter. The main source factors for fine particles were secondary aerosol, the electroplating industry, vehicle emissions, and biomass burning. *Santoso et al.* [2008] showed that biomass burning contributed to 40% of the $PM_{2.5}$ mass in suburban areas and 20% of the $PM_{2.5}$ mass in urban areas in Bandung Indonesia.

Following a critical review of the literature, it was seen that the chemical signatures of $PM_{2.5}$ to identify the potential sources during the southwest monsoon were lacking. There is also a need to improve understanding of the impact of atmospheric reactive gases, the effect of physical meteorological factors, wildfires, the burning of agricultural waste and peat soil, and combustion and noncombustion activities in an urban setting, on the alteration of the concentrations and compositions of aerosol particles. This study focuses on

the comprehensive analysis of water-soluble ions (WSIs), trace species, rare earth elements (REEs), and a range of elemental and organic carbon (EC and OC) compounds in $PM_{2.5}$ coupled with the concentration of reactive gases, meteorological driving factors, and biomass or wildfire hotspots. Therefore, the objectives of this study are to characterize $PM_{2.5}$ in Malaysia during the southwest monsoon, taking into consideration $PM_{2.5}$ concentrations, chemical compositions, and the concentrations of reactive gases. These characteristics vary due to changes in physical driving factors and sources, and the correlations between them will identify the potential sources. PMF, potential source contribution function (PSCF), and biomass fire hotspots will be used to determine the $PM_{2.5}$ factors and source locations to gain a greater understanding of the aerosol emissions during the dry season of the southwest monsoon.

2. Material and Methods

2.1. Sampling Site

This study was conducted on the rooftop of the Biology Building (a five-story building) at the Faculty of Science and Technology, Universiti Kebangsaan Malaysia (UKM), at about 65 m above sea level. This is a semi-urban area and located around 20 km to the south of central Kuala Lumpur. The nearest main roads are about 300 m from the sampling location and predominantly used by light-duty vehicles. The two nearest highways (the North-South Highway and the Silk Highway), which are about 2 km away from the monitoring site, are used by both heavy-duty and light-duty vehicles. In addition, the site itself is surrounded by dense forest. The gridded emissions of $PM_{2.5}$ ($t\,yr^{-1}$) as reported by *Zhang et al.* [2009] is shown in Figure 1a, and its emission around the sampling site is comparable to some parts of south China, particularly Guangdong (about 10,000 $t\,yr^{-1}$).

2.2. Sampling Protocol and Chemical Analysis

The daily $PM_{2.5}$ samples (24 h) were collected on quartz microfiber filters (203 mm × 254 mm; Whatman™, UK) using a high-volume sampler (HVS; Tisch, USA). As part of the preparation, the filters were baked at 500°C for 3 h to remove any deposited organic compounds. Prior to weighing, the blank filters were conditioned in desiccators for 24 h to ensure the equilibrium of mass concentration. After the collection of samples, a similar procedure was followed for the exposed filter papers. The filter papers were weighed using a five-digit, high-resolution electronic balance (A&D, GR-202, Japan) with a 0.01 mg detection limit. The filter samples were then refrigerated at −18°C until the extraction was carried out. In total, 39 samples of $PM_{2.5}$ were collected from 24 June to 14 September 2014 to coincide the southwest monsoon. The samples were collected on a random basis during the entire sampling period. The measurement of particle number concentration (PNC) was performed using a multichannel environmental dust monitor (Grimm EDM 180, Grimm Aerosol Technik, Germany). The built-in aerosol spectrometer employs a state-of-the-art optical particle counter for the in situ measurement of PNC ranging between 0.27 μm and 34 μm [*Grimm and Eatough*, 2009; *Weber et al.*, 2010; *Xiaoai et al.*, 2010]. Data were recorded at 1 min intervals. Then, the particle mass of PM_1 (aerodynamic diameter of less than or equal to 1 μm), $PM_{2.5}$ (aerodynamic diameter of less than or equal to 2.5 μm), PM_{10} (aerodynamic diameter of less than or equal to 10 μm), and total suspended particulate matter were obtained by applying the theoretical mass equation and the measurement principle based on the light-scattering technology for single-particle counts [*Grimm and Eatough*, 2009; *Technik*, 2006]. In the conversion process, particle diameter data were first converted into particle volume using the mean particle diameter between the thresholds of the 31 different channels. This volume data were converted into the mass distribution of particles using a density factor which Grimm had established as an "urban environment" factor [*Grimm and Eatough*, 2009].

For WSIs and trace species analyses, a portion of the filter samples was cut into small pieces and placed directly into 50 mL centrifuge tubes containing ultrapure water (18.2 MΩ cm; EASYpure® II, Thermo Scientific, Canada). The extraction process involved ultrasonic vibration, centrifuge, and mechanical shaking. The samples were first sonicated in an ultrasonic bath (Elmasonic S70H, Elma, Germany) for 20 min, and then the extraction solutions were centrifuged at 2500 rpm (Kubota 5100, Japan) for 10 min before being shaken using a vortex mixer for 10 min. The sonication and centrifuge steps were repeated twice before the extract was filtered using glass microfiber filters (Whatman™, UK). Both the trace species and the water-soluble ion extract samples were refrigerated at 4°C until further analysis. The trace species (Al, Ba, Ca, Fe, Mg, Pb, Zn, Ag, As, Cd, Cr, Li, Be, Bi, Co, Cu, Mn, Ni, Rb, Se, Sr, and V) and REE (In, Tl, U, Ce, Dy, Er, Eu, Gd, Ho, La, Lu, Nd, Pr, Sc, Sm, Tb, Th, Tm, Y, and Yb) were determined through inductively

Table 1. Summary Results of $PM_{2.5}$ ($N = 39$), Its Selected Compositions, and PNC During the 2014 SEA Dry Season (Southwest Monsoon)

Variables	Unit	Mean ± STDEV	Minimum	Maximum	5 (%)	95 (%)	MDL[a]
$PM_{2.5}$	$\mu g\,m^{-3}$	18.3 ± 11.8	6.64	68.2	8.76	29.8	-
TC	$\mu g\,m^{-3}$	6.14 ± 6.55	1.45	39.6	2.24	11.4	-
OC	$\mu g\,m^{-3}$	4.63 ± 6.06	0.73	36.3	1.28	9.14	-
EC	$\mu g\,m^{-3}$	1.51 ± 0.85	0.52	3.35	0.67	3.12	-
Na^+	$\mu g\,m^{-3}$	0.14 ± 0.06	0.05	0.30	0.06	0.20	0.034
NH_4^+	$\mu g\,m^{-3}$	0.54 ± 0.43	0.06	1.93	0.14	1.11	-
K^+	$\mu g\,m^{-3}$	0.21 ± 0.12	0.00	0.56	0.13	0.41	0.016
Ca^{2+}	$\mu g\,m^{-3}$	0.20 ± 0.12	0.02	0.64	0.07	0.37	0.0015
Mg^{2+}	$\mu g\,m^{-3}$	0.06 ± 0.09	0.00	0.39	0.01	0.22	0.006
F^-	$ng\,m^{-3}$	3.10 ± 3.88	0.25	13.3	0.49	12.3	0.0068
Cl^-	$ng\,m^{-3}$	23.0 ± 24.2	3.44	120	7.13	49.7	0.0265
NO_3^-	$\mu g\,m^{-3}$	0.28 ± 0.17	0.11	0.94	0.13	0.51	0.0477
PO_4^{3-}	$ng\,m^{-3}$	113 ± 100	0.12	342	11.7	271	0.135
SO_4^{2-}	$\mu g\,m^{-3}$	1.98 ± 1.19	0.46	5.31	0.81	3.44	0.0128
Al	$ng\,m^{-3}$	11.9 ± 7.97	0.29	31.4	3.30	25.5	0.335
Fe	$ng\,m^{-3}$	5.67 ± 4.09	0.14	18.1	1.82	10.1	1.01
Zn	$ng\,m^{-3}$	15.8 ± 11.5	0.09	68.6	7.74	29.5	0.338
Mn	$ng\,m^{-3}$	1.19 ± 0.67	0.33	3.75	0.50	2.33	0.029
Mg	$ng\,m^{-3}$	8.48 ± 3.87	2.36	17.0	3.59	13.6	3.32
As	$ng\,m^{-3}$	3.29 ± 2.95	0.02	14.5	0.68	7.12	0.008
Ba	$ng\,m^{-3}$	0.94 ± 0.60	0.29	2.88	0.43	1.46	0.092
Bi	$ng\,m^{-3}$	0.08 ± 0.08	0.01	0.39	0.01	0.16	0.0004
Cd	$ng\,m^{-3}$	0.21 ± 0.13	0.07	0.63	0.10	0.37	0.004
Co	$ng\,m^{-3}$	0.01 ± 0.01	0.00	0.03	0.00	0.02	0.003
Cs	$ng\,m^{-3}$	0.03 ± 0.02	0.00	0.10	0.02	0.06	0.001
Cu	$ng\,m^{-3}$	2.46 ± 2.25	0.01	12.8	0.95	4.39	0.014
Ga	$ng\,m^{-3}$	0.02 ± 0.02	0.01	0.09	0.01	0.04	0.001
K	$ng\,m^{-3}$	120 ± 76.2	30.2	387	66.5	188	12.6
Ni	$ng\,m^{-3}$	0.73 ± 0.44	0.10	2.36	0.21	1.25	0.036
Pb	$ng\,m^{-3}$	4.54 ± 3.75	0.01	16.2	0.54	9.13	0.013
Rb	$ng\,m^{-3}$	1.06 ± 0.73	0.01	3.44	0.54	1.73	0.012
Se	$ng\,m^{-3}$	0.37 ± 0.26	0.03	1.23	0.15	0.59	0.051
Tl	$ng\,m^{-3}$	0.03 ± 0.02	0.01	0.09	0.01	0.06	0.0004
V	$ng\,m^{-3}$	1.31 ± 1.03	0.00	4.47	0.08	2.69	0.004
PNC (0.27–34 μm)	$\#\,cm^{-3}$	265 ± 210	1.00	1540	84.9	489	-
PNC (<1 μm)	$\#\,cm^{-3}$	265 ± 210	20.5	1530	84.2	488	-

[a]The unit for MDL is $ng\,m^{-3}$.

coupled plasma–mass Spectrometry (ICP-MS; PerkinElmer ELAN 9000, USA). The method detection limit (MDL) for trace species was calculated as 3 times the standard deviation of three replicates of the filter blanks. Overall, MDL was as reported in Table 1. During the trace species and REE analysis by ICP-MS, two modes of analysis were applied with updated calibration curves each time. Based on trial runs, the elements were initially screened for concentration levels, which resulted in two modes analysis: (a) a set of metals with high concentrations (with several dilution factors; Al, Ca, Fe, Mg, Zn, and Mn), and (b) a set of metals with low concentrations (Ba, Pb, Ag, As, Cd, Cr, Li, Be, Bi, Co, Cu, Ni, Rb, Se, Sr, and V), as described in our previous paper [*Khan et al.*, 2016a]. Multi-Element Calibration Standards 2 and 3 (PerkinElmer Pure Plus; PerkinElmer, USA) were used as calibration standards.

The WSI compositions (Na^+, NH_4^+, K^+, Ca^{2+}, Mg^{2+}, Cl^-, NO_3^-, and SO_4^{2-}) were determined using ion chromatography (IC) (Metrohm 850 model 881 Compact IC Pro, Switzerland). Metrosep A-Supp 5–150/4.0 and C4–100/4.0 columns were used to determine cations and anions, respectively. The 1.7 mmol L^{-1} nitric and 0.7 mmol L^{-1} dipicolinic acids were prepared for use as eluents for cations. Eluents of 6.4 mmol L^{-1} sodium carbonate (Na_2CO_3) (Merck, Germany) and 2.0 mmol L^{-1} sodium bicarbonate ($NaHCO_3$) (Merck, Germany) were prepared and used to measure anions (Cl^-, NO_3^-, and SO_4^{2-}) with a flow rate of 0.7 mL min^{-1}. The 100 mmol L^{-1} Suprapur® sulfuric acid (H_2SO_4) (Merck, Germany) was also prepared to use as a suppressor regenerant, and ions were detected by a conductivity detector.

A thermal/optical carbon analyzer from the Desert Research Institute (DRI) was used to determine the elemental (EC1, EC2, and EC3) and organic (OC1, OC2, OC3, and OC4) fractions from the $PM_{2.5}$ fraction (DRI model 2001, USA). This method is based on the thermal/optical reflectance procedure described as IMPROVE A PROTOCOL [*Fujii et al.*, 2014]. The filter blanks ($N = 4$) collected on 29 June, 6 July, 17 July, and 14 September 2014 were also analyzed. It is necessary to note that the field-based filter blanks were loaded into the HVS without it being turned on and kept in the HVS for 24 h, similar to the duration for the samples of this campaign. The purpose of the field blanks was to make deductions with regard to (a) contamination from the filter materials and (b) gas phase adsorption of volatile organics. The mass concentrations of OC and EC for each sample were corrected for the blanks. As per IMPROVE A PROTOCOL [*Fujii et al.*, 2014], OC fractions were measured in the presence of He and at temperature spans of 25–140°C (OC1), 140–280°C (OC2), 280–480°C (OC3), and 480–580°C (OC4). EC fractions were measured in the presence of He/O_2 and at temperature spans of 580°C (EC1), 580–740°C (EC2), and 740–840°C (EC3). During the measurements of OC and EC, some portions of OC behaved like EC and produced a peak in the split of OC and EC. This OC is known as the pyrolyzed OC and is reported as OP when measured in the presence of He. *Miyazaki et al.* [2007] and *Yu et al.* [2002] define this carbon fraction as (i) carbon that may be originally refractory and associated with high molecular weight (MW) compounds and/or (ii) carbon that may undergo pyrolysis during the thermal analysis followed by evolution in the He mode prior to the He/O_2 mode. The pyrolyzing effect mainly occurred in the helium mode, and the OC will be partly pyrolyzed and resistant to volatilization in the He mode [*Kondo et al.*, 2011; *Novakov et al.*, 2000]. The OC reported in this study was defined with the following equations:

$$OC = OC1 + OC2 + OC3 + OC4 + OP \tag{1}$$

EC was estimated as

$$EC = EC1 + EC2 + EC3 - OP \tag{2}$$

Total carbon (TC) was described as

$$TC = EC + OC \tag{3}$$

where OP is defined as the pyrolyzed OC evolved in the He mode.

The secondary organic carbon (SOC) was estimated using the lowest ratio value of OC to EC (OC/EC). *Khan et al.* [2010b] reported that the minimum ratio line in the OC-EC plot is a constant mixture of primary EC and OC, while *Harrison and Yin* [2008] described the points above the minimum ratio line as representing the additional OC formed from secondary origins. This EC-tracer method has been widely used to distinguish primary OC from SOC [*Carvalho et al.*, 2006; *Castro et al.*, 1999; *Duarte et al.*, 2008; *Khan et al.*, 2010b; *Pio et al.*, 2011; *Turpin and Huntzicker*, 1991, 1995; *Turpin and Lim*, 2001]. It was assumed that EC and OC were measured in ambient air where primary combustion was dominant and photochemical activities were weak [*Turpin and Huntzicker*, 1991]. The SOC estimation was calculated as

$$SOC = OC_{total} - \left[\left(\frac{OC}{EC} \right)_{min} \times EC \right] \tag{4}$$

where the minimum OC/EC ratio was 0.55, which is believed to be emitted from stable primary common combustion sources (e.g., combustion and resuspension of combustion particles) and season dependent [*Yuan et al.*, 2006]. *Safai et al.* [2014] observed 0.49 as the minimum OC/EC ratio during the monsoon (wet season) in Pune, India, whereas *Huang et al.* [2014] found a similar value during the summer in Hong Kong. However, this method has significant ranges of uncertainty, since the ratios of OC/EC can be influenced by various factors such as meteorology, diurnal and seasonal fluctuations in emissions, local sources, and long-range transport, which vary considerably [*Duan et al.*, 2007]. In this study, all samples were collected in a similar manner, i.e., 24 h sampling in one season, which reduces the uncertainty of the estimation. In addition, the lowest value of OC/EC was used to represent the primary combustion source.

2.3. Multivariate Receptor Modeling Technique

SA analysis was conducted using the U.S. Environmental Protection Agency (EPA) PMF version 5.0 model as suggested by *Norris et al.* [2014]. PMF is a factor-based receptor model that decomposes a matrix of sample

data into two matrices, i.e., chemical compositions and the contribution of each factor to each sample. Mathematically, PMF can be defined as equation (5)

$$X_{ij} = \Sigma_{K=1}^{P} g_{ik} f_{kj} + e_{ij} \tag{5}$$

where X_{ij} is the concentration of jth species of the ith sample, p is the number of factors, g_{ik} is the contribution of kth factor of the ith sample, f_{kj} is the factor profile of jth species of the kth factor, and e_{ij} is the residual matrix for the jth species measured in the ith sample.

The PMF solution minimizes the objective function Q with the adjusted values of g, f, and p. Q is defined by equation (6)

$$Q(E) = \Sigma_{i=1}^{m} \Sigma_{j=1}^{n} \left[\frac{e_{ij}}{s_{ij}}\right]^2 = \Sigma_{i=1}^{m} \Sigma_{j=1}^{n} \left[\frac{X_{ij} - \Sigma_{k=1}^{p} g_{ik} f_{kj}}{s_{ij}}\right]^2 \tag{6}$$

where S_{ij} is an estimate of the uncertainty of the jth species in the ith sample. PMF 5.0 operates in a robust mode by default, which downweighs the outliers affecting the fitting of the contributions and profiles. PMF uses two data files as input for each sample: (1) concentration and (2) uncertainty. The concentration of each element was pretreated and validated based on noisy data or outliers, missing values, and/or values below the MDL. The variables with outliers were excluded if present [*Baumann et al.*, 2008; *Polissar et al.*, 1998a; *Polissar et al.*, 1998b]. The second data file is the uncertainty value of each variable by each sample. Due to the lack of availability of measurements or methodological data to calculate errors, the following empirical equation (equation (7)) was used to estimate the error of the species concentration:

$$S_{ij} = \overline{X}_J \times C_1 + X_{ij} \times (C_1 + C_2) \tag{7}$$

where X_{ij} is the observed concentration of species and $\overline{X}_j$ is the mean value of each element. C1 and C2 are the empirical constants and the value usually between 0.01 and 0.05 and between 0.1 and 0.5 for C1 and C2, respectively. In this work, the values of C1 and C2 were chosen to determine the most meaningful and physically interpretable solution using a trial-and-error approach [*Ogulei et al.*, 2006a, 2006b], as summarized in Figures S1 and S2 in the supporting information.

In addition, we applied a similar step to values below the detection limit. *Harrison et al.* [2011] and *Hedberg et al.* [2005] applied this procedure for uncertainty estimations in their studies. In the PMF 5.0 procedure, we selected the values of 0.02 and 0.35 for C1 and C2, as the end calculation was optimized with lower error (%) and the Q true/Q exp with these values. An additional 5% uncertainty was added to account for methodological errors in the preparation of filter papers, gravimetric mass measurements, and the preparation of the calibration curves. The model output of source contributions is normalized or dimensionless (average of each factor contribution is 1). Therefore, the mass concentrations of the identified sources were scaled using the following multiple linear regression (MLR) analysis (equation (8)):

$$M_i = S_0 + \sum_{k=1}^{p} S_k g_{ik} \tag{8}$$

where M_i is the concentration of the total concentration of PM$_{2.5}$ in ith sample, S_k is the scaling constant, S_0 is the regression constant, and g_{ik} is the source contribution found in the result of PMF modeling. After the run of MLR, the coefficient of determination (S_k) multiplied with the respective factor contribution to convert them into the mass concentration ($\mu g \, m^{-3}$). Several other researchers have successfully applied this MLR approach to express the output of PMF [*Amil et al.*, 2016; *Callén et al.*, 2014; *Hedberg et al.*, 2005; *Khan et al.*, 2012, 2015c, 2016a].

The variables included were PM$_{2.5}$, Al, Ba, Fe, Mg, Pb, Zn, As, Cd, Ga, K, Bi, Co, Cu, Cs, Mn, Ni, Rb, Se, V, Tl, Na$^+$, NH$_4^+$, K$^+$, Ca^{2+}, Mg^{2+}, F$^-$, Cl$^-$, NO$_3^-$, SO$_4^{2-}$, OC, EC, and OP. The variables were accepted for further feeding into the PMF model on consideration of the following criteria: (a) species with more than 50% of the data below MDL were excluded; (b) any missing values were replaced with the median of each variable; (c) for the signal-to-noise (S/N) ratio, variables with ratios of $0.2 \leq S/N < 1$ were set as "weak" species, while the rest were categorized as "strong" species (S/N > 1)[*Heo et al.*, 2009; *Richard et al.*, 2011; *Yu et al.*, 2013]; (d) the percentage of missing data; (e) exclusion of variables with noisy or outlier data—the PM$_{2.5}$ mass was also categorized as weak so as not to affect the PMF solution; and (f) the stability of the bootstrap replicate data to the base run. The base model run was executed to find the global Q value minima with different numbers of factors. A detail of the selection of the number of factors is reported in the supporting information. After
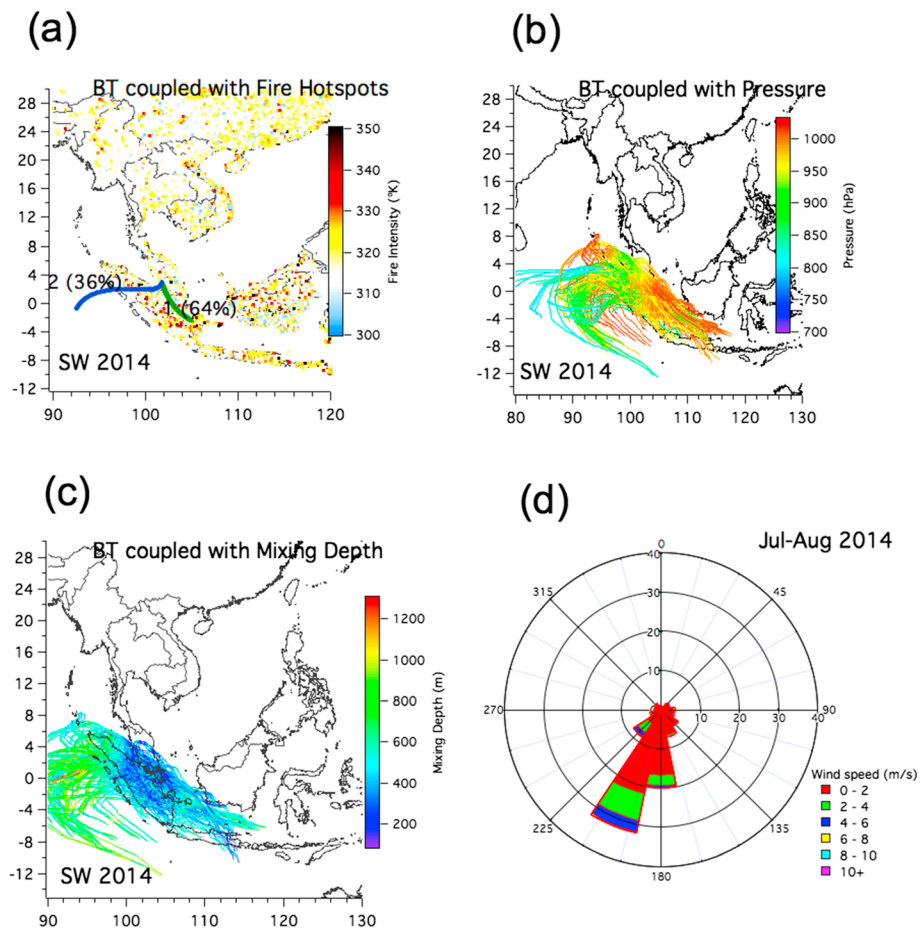
Figure 2. Backward trajectory (BT) for 120 h starting from 16:00 UTC and released at the height of 500 m coupled with (a) biomass fire hotspots, (b) pressure gradient, (c) mixing depth (m), and (d) a depiction of wind speed and wind direction in summer 2014.

increasing and decreasing the number of factors, a procedure introduced by *Fang et al.* [2015], there was no complete separation of the coupled sources as demonstrated in Figure S1. The rotation function F_{peak} was also considered in the range of -1.0 to 1.0, and $F_{peak} = 0$ was accepted to further evaluate the results as the unrotated output was deemed reasonably meaningful (Figure S2). Therefore, we decided that the seven-factor solution was the most physically meaningful after we carefully considered the five-, six-, and seven-factor solutions (Figures S3–S8). A more detailed discussion of the methodology and optimization of the number of factors can be found in the supporting information [*Brown et al.*, 2015; *Fang et al.*, 2015; *Ogulei et al.*, 2006a, 2006b; *Paatero et al.*, 2014].

2.4. Backward Trajectories, Potential Source Contribution Function and Local Circulation, and Aerosol System

The backward trajectories (BTs) were calculated in order to identify the transport pathways of air masses to the sampling site. The Hybrid Single-Particle Lagrangian Integrated Trajectory version 4.9 (HYSPLIT 4.9) was used to calculate the 120 h air mass BT [*Rolph*, 2015]. Mean clusters as well as integrated BT are shown in Figures 2a and 2b, respectively.

The basic PSCF can be defined with the following equation [*Ashbaugh et al.*, 1985; *Hopke et al.*, 1995; *Malm et al.*, 1986]:

$$PSCF_{ij} = \frac{m_{ij}}{n_{ij}} \qquad (9)$$

For a gridded cell i by j array, n_{ij} is the number of endpoints which fall into the ijth cell and m_{ij} is the number of endpoints among the n_{ij} corresponding to the trajectories that arrive at the receptor location with the
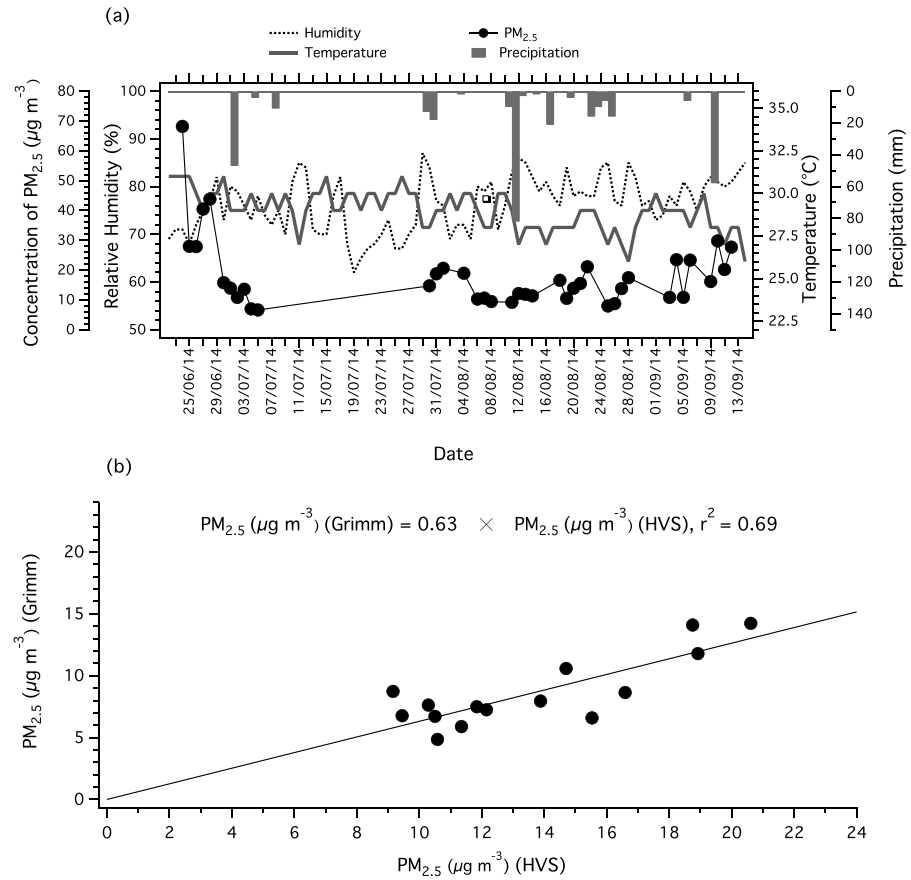
Figure 3. (a) Time series of 24 h mean concentration of $PM_{2.5}$, relative humidity, ambient temperature, and precipitation and (b) a correlation plot of $PM_{2.5}$ (HVS) with $PM_{2.5}$ (Grimm).

concentration of the pollutant exceeding a predefined threshold value. To minimize the influence of the grid cells with small n_{ij}, an arbitrary weighted function was created to reduce the PSCF values for the particular cells [*Hopke et al.*, 1995; *Xie et al.*, 1999]. For this study, we divided the region of interest into areas of $0.5° \times 0.5°$ resolution covered by the trajectories. The potential sources of $PM_{2.5}$ are likely to demonstrate a location with a high PSCF value due to the transport of $PM_{2.5}$ by an air parcel to the sampling site. Furthermore, the PSCFs are used to identify the likely source regions and pathways of distant pollutants sources as described by *Ashbaugh et al.* [1985], *Begum et al.* [2005], *Hopke et al.* [1995], *Malm et al.* [1986], and *Zeng and Hopke* [1989]. Several researchers have successfully applied PSCF to infer source regions [*Begum et al.*, 2005; *Choi et al.*, 2013; *Heo et al.*, 2009; *Zhang et al.*, 2013].

HYSPLIT was run for every day in the sampling period, from 24 June to 12 September 2014. The 48 h trajectories with a 1 h interval were selected. The increase of trajectory duration during the entire period may have led to an unrealistic source location. Further, a weighting function W_{ij} was multiplied by the PSCF value to reduce the effect of large ratios with high uncertainty in grid cells resulting from small values of n_{ij}:

$$W_{ij} = \begin{cases} 1 & 9 < n_{ij} \\ 0.9 & 8 < n_{ij} \leq 9 \\ 0.8 & 7 < n_{ij} \leq 8 \\ 0.7 & 8 < n_{ij} \leq 7 \\ 0.6 & 7 < n_{ij} \leq 6 \\ 0.5 & 6 < n_{ij} \leq 5 \\ 0.4 & 5 < n_{ij} \leq 4 \\ 0.3 & 4 < n_{ij} \leq 3 \\ 0.2 & 3 < n_{ij} \leq 2 \\ 0.1 & 2 < n_{ij} \leq 1 \end{cases} \tag{10}$$

Aerosol optical depth (AOD) at 550 nm was downloaded from the Giovanni web portal of the National Aeronautics and Space Administration. This is the daily level 3 data from the Moderate Resolution Imaging Spectroradiometer (MODIS) Terra and Aqua (dark target; MOD08_D3 v051) for June–September 2014, with a spatial resolution of $1° \times 1°$. To obtain the climatology of the mean AOD representing the Malaysian Peninsula region, the area average of the AOD data at 80°E–130°E, −15°N–30°N was first calculated and then was averaged across time. The 10 m above surface wind vector data with a resolution of $0.25° \times 0.25°$ were downloaded from European Centre for Medium-Range Weather Forecasts website, and the climatological mean of the wind vector for the same period was calculated and overlaid on the AOD data as shown in Figure 1b. The AOD around the sampling site was lower compared to the South Sumatra region. During this period, wind predominantly blew from the southwest region. Therefore, our hypothesis is that the downwind area source could influence the aerosol pollution at the sampling site. Also, the boundary layer height (BLH) is slightly higher in North Sumatra and nearly the same in South Sumatra when compared to the sampling region (Figure 1c).

3. Results and Discussions

3.1. Atmospheric Aerosol Load and Impact of Backward Trajectories and Meteorological Factors

Figure 3a shows the variation of $PM_{2.5}$ concentration with respect to rainfall, relative humidity, and temperature. The concentration of $PM_{2.5}$ was relatively high in the fourth week of June and then dropped during the first week of July. The concentration of $PM_{2.5}$ slightly increased again during the first and second weeks of September, and the precipitation was inversely proportionate to the level of $PM_{2.5}$. During the southwest monsoon, the relative humidity was lower than 90%. The temperature was found to vary in the range of 26–32°C. Rainfall events in this season were relatively short, as shown in Figure 3. The climate in SEA is strongly influenced by the changes in the monsoonal seasons [*Juneng et al.*, 2009, 2011]. The local climate can be divided into four different seasons: (i) southwest monsoon (June–September), (ii) northeast monsoon (December–March), (iii) intermonsoon I (April–May), and (iv) intermonsoon II (October–November).

During the southwest monsoon, which is usually associated with the dry season, a high density of biomass fire or wildfires hotspots were reported in the upwind of the sampling location [*Khan et al.*, 2015a, 2015b, 2015c, 2016a; *Sahani et al.*, 2014]. The dominant boundary-transported air was from the South Sumatra region. This was largely due to the local wind pattern, which was predominantly southwesterly as shown in Figure 2d, in addition to the fire hotspots, which were densely distributed in the BT region. The wind rose plot was consistent with the responses of the BT. During the northeast monsoon, which usually corresponds to the wet season, the wind was predominantly blowing from the northeast direction, from the South China Sea. This northeasterly wind would bring along a large amount of moisture from the ocean, which would have caused heavy rainfall over the east coast region of Peninsular Malaysia.

As shown in Table 1, the $PM_{2.5}$ concentration varies from 6.64 to 68.2 $\mu g\,m^{-3}$ with a mean value of 18.3 $\mu g\,m^{-3}$. The 24 h average concentration of $PM_{2.5}$ was lower than the 35 $\mu g\,m^{-3}$ U.S. EPA National Ambient Air Quality Standard (NAAQS), the 25 $\mu g\,m^{-3}$ WHO 24 h guideline, and the 75 $\mu g\,m^{-3}$ 24 h the New Malaysia Ambient Air Quality Standard (NMAAQS) for $PM_{2.5}$ (Interim 1-2015). However, the results showed that 8%, 18%, and 3% of the $PM_{2.5}$ samples exceed the NAAQS, WHO guideline, and NMAAQS, respectively. *Khan et al.* [2016a] reported a higher mean concentration of $PM_{2.5}$ (22.15 $\mu g\,m^{-3}$) during the 2013 dry season for the same site (UKM, Bangi). Higher $PM_{2.5}$ concentrations during the dry period in 2013 were due to the occurrence of a strong haze event [*Forsyth*, 2014]. In 2014, the haze event was not as severe. Studies conducted in other cities in Peninsular Malaysia during the same season showed varied concentrations. For example, the west of the peninsular showed higher concentrations, while sites on the east coast of the peninsular reported lower concentrations of $PM_{2.5}$ [*Keywood et al.*, 2003; *Mohd Tahir et al.*, 2013; *Rahman et al.*, 2011]. In comparison to other Asian cities during the dry southwest season, the $PM_{2.5}$ concentrations in this study were much lower. The $PM_{2.5}$ concentration was 50 $\mu g\,m^{-3}$ for Bangkok, 168 $\mu g\,m^{-3}$ for Beijing, 46 $\mu g\,m^{-3}$ for Chennai, 53 $\mu g\,m^{-3}$ for Bandung, 44 $\mu g\,m^{-3}$ for Manila, and 124 $\mu g\,m^{-3}$ for Hanoi based on the samples collected in 2001–2004 as reported by *Kim Oanh et al.* [2006]. However, the $PM_{2.5}$ concentrations in the urban area of Bandung and the suburban location in Lembang of Indonesia were much lower compared to this study [*Santoso et al.*, 2008].
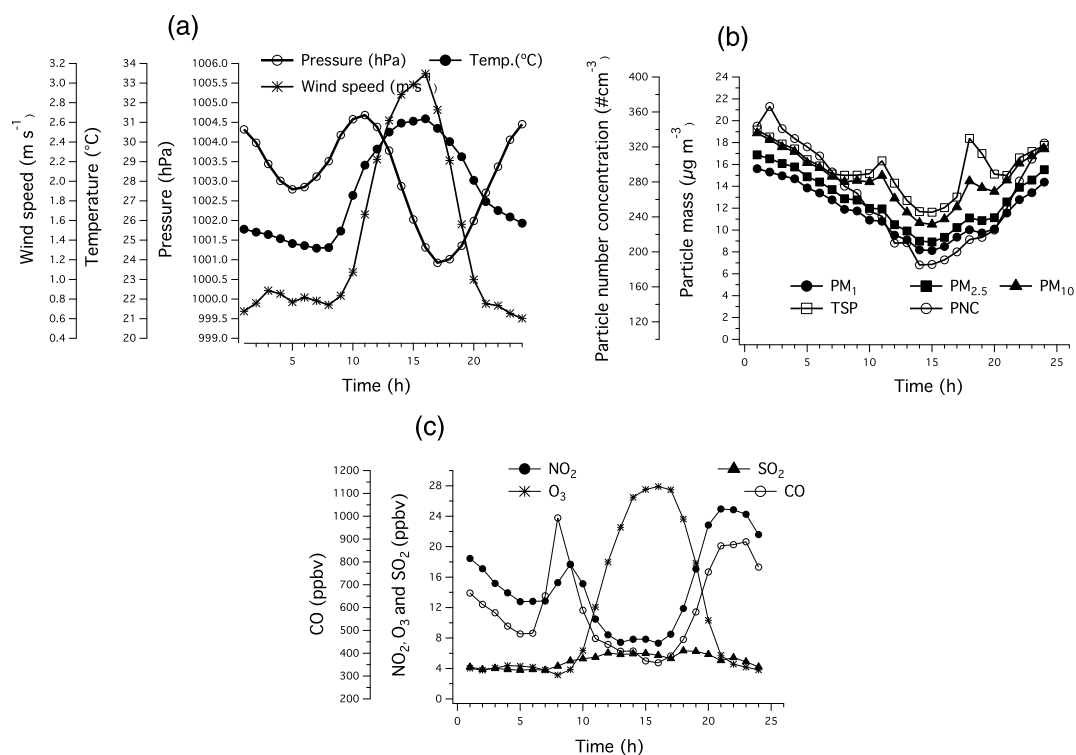
Figure 4. Diurnal cycle of (a) wind speed, temperature, and pressure; (b) PNC and particle mass concentration estimated (TSP, PM_{10}, $PM_{2.5}$, and PM_1); and (c) reactive gases (CO, NO_2, O_3, and SO_2).

3.2. Diurnal Variations of PNC, Particle Mass, Gases, and Meteorological Factors

The diurnal variations of temperature, wind speed, and pressure are presented in Figure 4a. Ambient temperature (°C) gradually increased from 21 to 22°C at 8.00 LT to reach a peak of 34°C at 16:00 LT and returned to 21–22°C from 20:00 to 8:00 LT. The wind speed (m s^{-1}) followed a similar unimodal distribution to ambient temperature. However, the pressure gradient showed a bimodal variation over a day. The high pressure was high at 11:00, while low-pressure region occurred at 17:00. The above diurnal scenarios are interrelated and largely govern the concentration of aerosol pollutants. The diurnal variations of particle mass and PNC show that the concentration of the aerosol particles decreased to the lowest level at about 15:00 and reached an apex at about 01:00. Three factors are significant in explaining the high concentration of particle mass and PNC: (i) sea-land breeze bringing clean air during the daytime; (ii) the boundary layer mixing height, which usually increases in the middle of the day and leads to a reduced level of pollution; and (iii) the high wind speed at about 3 m s^{-1}, which disperses the aerosol pollution. The diurnal variations of CO and NO_2 showed two peak hours of 08:00–09:00 and 20:00–23:00. The peak in the morning clearly reflects the traffic rush hour, whereby the emissions from traffic largely contributed to the high concentrations of CO and NO_2. However, there were three possible reasons for the peak in the evening, namely, (i) the evening rush hour, (ii) lower wind speeds, and (iii) the reduction of the mixing height. Over the 24 h, the concentration of SO_2 did not show any significant diurnal variation. However, the O_3 level showed a large variation during the middle of the day (13:00–18:00), at a point where the intensity of the UV light is the greatest. Secondary O_3 can be formed in ambient air in the presence of NO_x, hydrocarbons, and UV light.

3.3. Chemical Composition of $PM_{2.5}$

In Table 1, the 24 h average concentrations of carbonaceous and inorganic aerosol are presented. The major ions were NH_4^+, K^+, Ca^{2+}, and Na^+, while dominant trace species were Zn, Al, Mg, and Fe. The average concentrations of OC and EC were 4.63 (0.73–36.3) and 1.51 (0.52–3.35) $\mu g\,m^{-3}$, respectively, with an average OC/EC ratio of 2.97 (range of 0.55–11.2). The 24 h concentration variations of OC1, OC2, OC3, OC4, OP, EC1-OP, EC2, and EC3 are shown in Figure 5. The concentrations of OC2 and OC3 were high on 24–28 June, 31 July to 2 August, and 10–12 September. OC3 was about 31% of the total OC, and
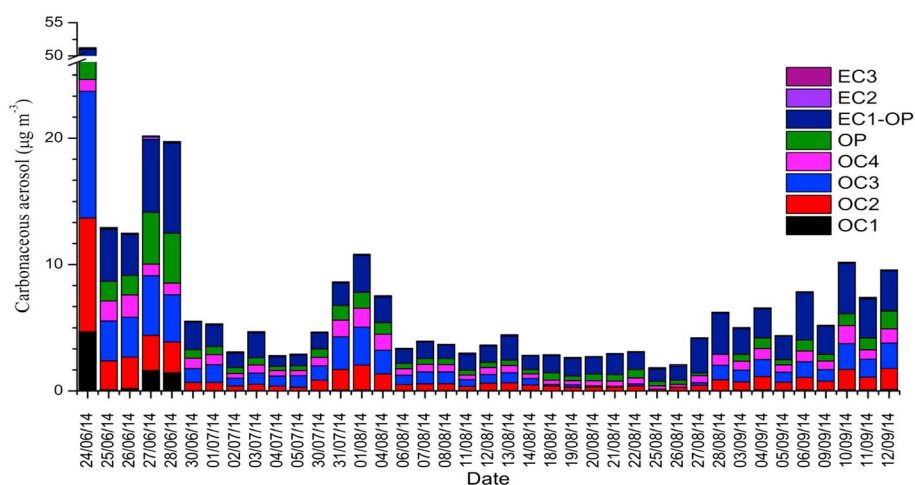
Figure 5. Time series of carbonaceous aerosol compositions (OC1, OC2, OC3, OC4, OP, EC1-OP, EC2, and EC3).

97% of EC was EC1-OP. The OP value was relatively high during 24–28 June, which is retained to provide resolution in the thermal optical split of OC and EC. As shown in Figure 2, the mixing depth during the dry season was about 200–400 m, which enhanced the high concentrations of the OC, EC, and OP. In addition, the stable atmospheric conditions during this time resulted in minimal dispersion of the aerosol.

As shown in Table 2, the average 24 h concentration of the estimated SOC was 3.91 $\mu g\, m^{-3}$ with a range of 0.37 to 34.6 $\mu g\, m^{-3}$, which is 85% of the total OC. Thus, the remaining 15% of OC may have been released from primary combustion sources. *Malm et al.* [1994] and *Mancilla et al.* [2015] applied a factor of 1.4 to convert OC to organic matter (OM). *Turpin and Lim* [2001] also suggested a value of 1.6 ± 0.2 for urban sites. In addition, a moderate correlation between CO and SOC ($R^2 = 0.69$, $p < 0.01$) suggests that the generation of SOC influences the emission of CO. The observation from Figure S9 is that OM and SOC proportionally covaried in June and July but that the concentration of SOC was almost stable in both August and September. The surface temperature was shown to be lower in these 2 months when compared to temperatures in June and July 2014 (Figure 3). The intensity of the biomass burning usually depends on the number of hotspots and the dry conditions. In 2014, this dry period was at its apex during June and July compared to August and September.

3.4. Correlation Among the Major Variables and the Mass Size Distribution of Aerosol Particles

Figures 6a–6l illustrate the correlations of PNC with CO and NO_2 for day (6:00 A.M. to 6:00 P.M.) and night data (6:00 P.M. to 6:00 A.M. the next day). The night data set of PNC-CO shows strong colinearity when compared to the day data points. However, the night data points of PNC-NO_2 do not show any consistent linearity. As shown in Figure 6, both OC and EC were significantly associated but poorly correlated ($R^2 = 0.33$, $p < 0.01$), suggesting that these two variables were not emitted consistently from a similar source. The mean OC/EC ratio was 2.97 with a range of 0.55 to 11.2. Other researchers have reported varied ratios of OC/EC. For example, a summertime ratio of 1.8 was reported for the urban site Chengdu City, China [*Tao et al.*, 2013], and a range of 1.3 to 3.9 for the OC/EC ratio during the summer in Rome, Italy [*Lonati et al.*, 2008]. Studies by *Cachier et al.* [1989] and *Watson and Chow* [2001] suggested ratio values of OC/EC of 2.7, 1.1, and 9.0 for coal combustion, motor vehicles, and biomass burning, respectively. The highest value recorded for OC/EC was 14.4, as reported by *Watson and Chow* [2001], which represents the contribution from biomass forest fire sources. A similar observation was made by *Cong et al.* [2015]. *Fujii et al.* [2016] proposed ratio values of OP to OC4 to represent biomass burning from Indonesian peat fires, which is a widely recognized contributor

Table 2. The Estimated Mass Fraction of SOC and OM in $\mu g\, m^{-3}$

Variables	Mean	Minimum	Maximum	STD[a]
SOC	3.91	0.37	34.6	5.86
OM	6.49	1.07	50.9	8.48

[a]STD stands for standard deviation.
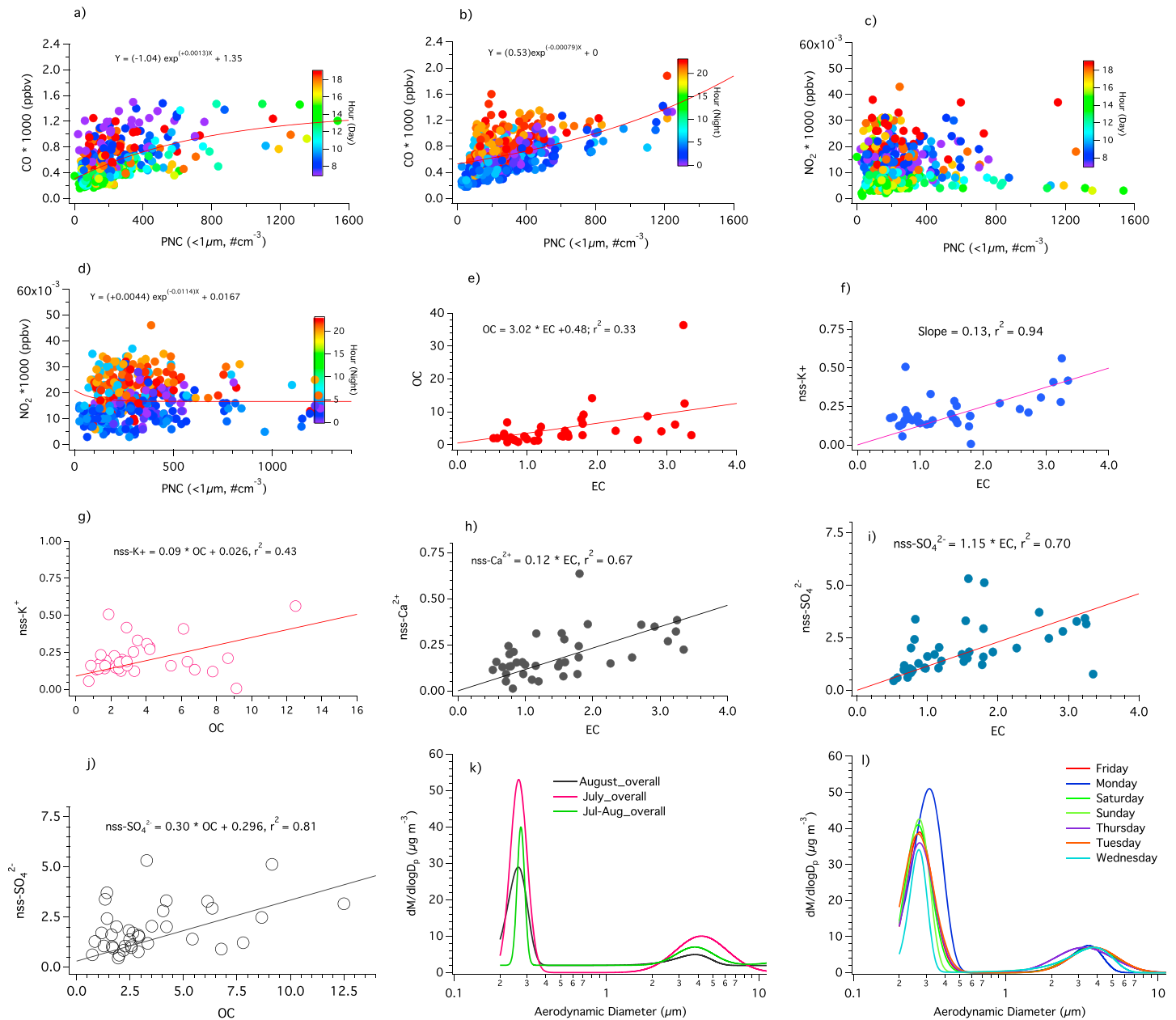
Figure 6. Correlation plots of $PM_{2.5}$ compositions, PNC, and size distribution of particle mass on basis of month and day of the week.

to aerosol pollution in the SEA region. Their study identified biomass burning as a haze event if OP/OC4 > 4 and a nonhaze event for OP/OC4 < 2. In this study, the average ratio of OP to OC4 was 1.48 with a range of 0.39 to 12.6. Between 24 and 30 June 2014, the OP/OC4 ratio was greater than 4 during a few sampling days, which clearly shows the appearance of haze on those days. Our average ratio of OP to EC was 0.68 with a range of 0.08 to 3.61, which also indicates that there were hazy days. Similar ratios were also reported by *Kondo et al.* [2011] in rural Guangzhou and Beijing and in Bangkok during biomass burning periods (0.23–0.28). They observed that the ratio of OP/BC was 0.04–0.08 in Tokyo, Jeju Island, and Bangkok during nonbiomass burning periods. Therefore, the observation from our results clearly demonstrates that some of the sampling days were greatly influenced by biomass burning sources. Non sea-salt K^+, Ca^{2+}, and SO_4^{2-} (nss-K^+ = [K^+] − [0.036 × Na^+], nss-Ca^{2+} = [Ca^{2+}] − [0.038 × Na^+], and nss-SO_4^{2-} = [SO_4^{2-}] − [0.252 × Na^+]) were estimated following the procedure explained by *Remoundaki et al.* [2013] and *Terzi et al.* [2010]. Correlation among them and others are demonstrated in Figures 6a–6k. As shown in Figure 6f, the strong

correlation between nss-K$^+$ and EC ($R^2 = 0.94$) supports the above argument. K$^+$ is a tracer widely reported in the literature as representing the biomass burning source [*Dai et al.*, 2013; *Heo et al.*, 2009; *Rahman et al.*, 2011; *Jun Tao et al.*, 2013]. As shown in Figure S10, SOC and CO showed a moderate correlation ($R^2 = 0.69$). EC and CO showed a poor correlation ($R^2 = 0.40$; Figure S11). Thus, the results of the correlation pairs indicate that motor vehicles have a moderate impact on the formation of SOC. However, a large portion of EC might be released by the biomass burning source during the dry season at this location. The strong correlation between nss-Ca^{2+} and OC indicates that they might link to a common source, but poor correlation between nss-Ca^{2+} and EC indicates a different origin for these variables. PM$_{2.5}$, captured by HVS, was moderately correlated ($R^2 = 0.69$) to PM$_{2.5}$ estimated by the Grimm Environmental Dust Monitor (Grimm180, Grimm Aerosol Technik, Germany). However, the correlation of the pair was significant ($p < 0.05$) as is shown in Figure 3b. Figures 6k and 6l show the size distribution of mass concentration by month and day of the week, respectively. The mass distribution of the smaller fraction (<300 nm) in July was stable compared to the standard deviation of the mass distribution in August. However, there was a shift of about 100 nm in mass mean diameter (MMD) to the coarse fraction of particulate matter in July 2014. On the other hand, the MMD was stable in fine and coarse modes for the comparison of the day of the week, excluding the MMD on Monday in the fine mode.

3.5. Source Apportionment by PMF 5.0 Receptor Modeling
3.5.1. Seven-Factor Solution for PM$_{2.5}$ Composition Data Set

To determine the source profiles for PM$_{2.5}$ at this site, U.S. EPA PMF 5.0, a robust receptor model, was applied using a data matrix of 39×33 (data points × variables). An optimum of a seven-factor result was chosen based on the most physically meaningful profiles. In the PMF solution, the f_{ij} matrix shows the "weight within the factor" of the constituents. Together with the dimensionless f_{ij} matrices, an "explained variation" (EV) shows the variance in the raw data set accounted for each factor [*Beddows et al.*, 2015]. Comparing the five-, six-, and seven-factor solutions, the major common sources were biomass burning coupled with sea salt, road dust and industrial emissions, coal-fired combustion, secondary inorganic aerosol (SIA) coupled with the F$^-$, and motor vehicle emissions coupled with sea salt. The final seven factors identified were (i) biomass burning coupled with sea salt [I], (ii) aged sea salt and mixed industrial emissions [I], (iii) road dust and fuel oil combustion, (iv) coal-fired combustion, (v) mineral dust, (vi) SIA coupled with F$^-$, and (vii) motor vehicle emissions coupled with sea salt [II], as demonstrated in Figure 7. Our results showed that the measured PM$_{2.5}$ concentrations and the predicted PM$_{2.5}$ were in good concordance (slope = 1.055, $R^2 = 0.89$; Figure 8a).

3.5.1.1. Factor 1: Biomass Fire Factor Coupled With Sea Salt [I]

The biomass burning factor was characterized by the presence of K$^+$, Ca^{2+}, Na$^+$, Cl$^-$, NO$_3^-$, and EC. K$^+$ is commonly used as a tracer for the biomass burning source [*Dall'Osto et al.*, 2013; *Kim and Hopke*, 2007; *Mustaffa et al.*, 2014; *Wahid et al.*, 2013]. Locally, a similar indication was used for the biomass burning source. For example, K in PM$_{2.5}$ measured by particle-induced X-ray emission was used for Kuala Lumpur [*Rahman et al.*, 2011]; K$^+$ by IC on the east coast of Malaysia [*Mohd Tahir et al.*, 2013]; and K$^+$ by IC [*Amil et al.*, 2016; *Khan et al.*, 2016a] for Kuala Lumpur and Bangi, Malaysia. Each year between June and September, Malaysia experiences dark haze episodes due to the burning of agricultural waste as well as natural forest fires in Indonesia. During this event, which sometimes prevails for several weeks, there were high concentrations of aerosol pollution and an associated reduction in visibility. A strong correlation ($R^2 = 0.94$) between nss-K$^+$ and EC verified that the tracers were released due to biomass burning. *Zhang et al.* [2010] also explained the biomass burning source as having a high contribution to EC. Other studies have also identified a biomass burning source of PM$_{2.5}$ with K, OC, and EC as tracers [*Hasheminassab et al.*, 2014; *Heo et al.*, 2009]. The ratio of OC/EC to this factor is 0.76. This value is much lower compared to the values of 1.2, 2.64, and 5.5 reported for the biomass burning source by *Cheng et al.* [2014], *Cheng et al.* [2011], and *Crutzen and Andreae* [1990], respectively. The BT analysis showed that the air mass was dominantly transported from the southwest region with the southwesterly wind originating from the biomass burning-prone areas. Meanwhile, the outdoor biomass fire count/locations traced by MODIS Aqua and Terra satellites appeared to relate to haze in SEA and neighboring regions, as shown in Figure 2a. *Reid et al.* [2013] reported a high intensity of fire counts in Indonesia during September, while *Khan et al.* [2015c] reported many hotspots in Thailand, Vietnam, and Laos during January to March. *Chang and Song* [2010] also reported that fire emissions were mainly concentrated in the same region, i.e., Indonesia, Thailand, Myanmar, and Cambodia. Biomass burning in Asia is the predominant source of trace gas and particulate matter. However, the season of biomass fires in
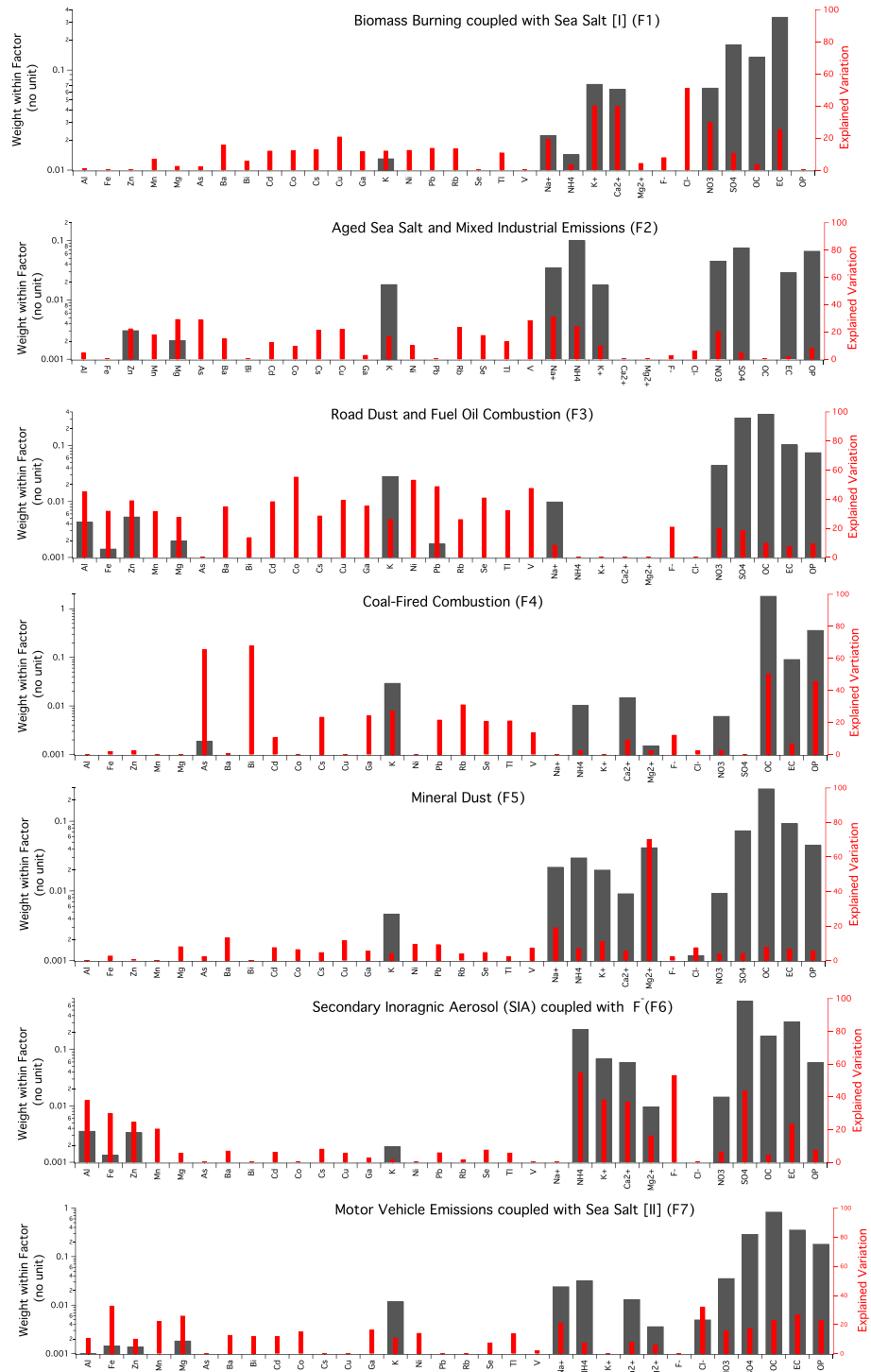
Figure 7. Source profiles of PM$_{2.5}$ predicted by PMF version 5.0.

Asia varies with the region. China was found to contribute 25% to the total biomass burning in Asia [*Streets et al.*, 2003] with Heilongjiang Province reported to have been seriously affected by forest fires between the years 2000 and 2011 [*Yang et al.*, 2013]. In addition, the suburbs of Shenzhen and the city center of Beijing were also reported as affected by biomass burning sources [*Dai et al.*, 2013; *L. Yu et al.*, 2013; *Zhang et al.*, 2013]. *Seneviratne et al.* [2011] reported that the main emission source for particulates in Colombo, Sri

Lanka, was biomass burning. In addition to biomass burning, this factor profile was also dominated by the Na^+ and Cl^- with 20% and 51% EVs, respectively, which supports the inclusion of a sea salt source. Overall, this factor contributed 7% of the estimated $PM_{2.5}$ concentration, as shown in Figure 8b.

3.5.1.2. Factor 2: Aged Sea Salt and Mixed Industrial Emissions

The aged sea salt factor was suggested by the dominance of Na^+ and NH_4^+ with Cl^- loss due to the displacement by acidic atmospheric gases. Studies by *Amil et al.* [2016], *Khan et al.* [2016a], *Khan et al.* [2010b], and *Mohd Tahir et al.* [2013] described chlorine deficiency under humid and high-temperature conditions. The aged sea salt factor was also identified by *Hasheminassab et al.* [2014], *Kim and Hopke* [2004], and *Ramadan et al.* [2000], who based this on the theory that the chlorine contribution to the aged sea salt factor is negligible. Studies by *Khan et al.* [2010b] and *Lestari and Mauliadi* [2009] identified the following reaction (equation (11)) behind the loss of Cl^- for Japanese and Indonesian sites, respectively:

$$H_2SO_4(aq) + 2NaCl(aq) \rightarrow Na_2SO_4(p) + 2HCl(g) \tag{11}$$
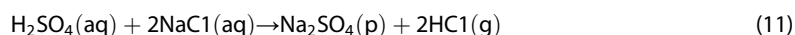
Song and Carmichael [1999] introduced the above mechanism which explains that the chlorine is depleted as sea salt reacts with the atmospheric gases, i.e., HCl and H_2SO_4, during transport when emitted from distant point sources. This source was predominant in the fourth week of June and the first week of September 2014 and accounted for 12% of the estimated $PM_{2.5}$ concentrations. In addition to sea salt tracers, this profile was dominated by Mn, Mg, V, As, Cs, and Cu. These metals are emitted by a range of industries such as metal-manufacturing industries and power plants [*Minguillón et al.*, 2014]. Overall, this source contributed to 5% of the estimated $PM_{2.5}$ concentrations.

3.5.1.3. Factor 3: Road Dust and Fuel Oil Combustion

Having a similar contribution to the estimated $PM_{2.5}$ concentrations as biomass fire at 7% this factor was characterized by high concentrations of Pb, Cu, Se, Cd, Al, Zn, and Co. Pb is seen in the literature as a tracer of motor vehicle sources [*Choi et al.*, 2013]. Although Pb had previously been added as an additive to gasoline fuel, this practice has been phased out in Malaysia since the 1980s. Consequently, *Khan et al.* [2016a] argue that Pb does not reflect the emissions from engine combustion but instead indicates non-exhaust traffic sources. Furthermore, the Pb source of $PM_{2.5}$ in Kuala Lumpur was detected in soil dust that had been contributed to by road dust [*Rahman et al.*, 2011]. Meanwhile, *Tao et al.* [2014] identified Pb in coal combustion. Cu is also associated with road dust released from nonexhaust car sources [*Amato et al.*, 2011; *Khan et al.*, 2016a], while *Wåhlin et al.* [2006] identified Cu to be emitted from the brake wear or the brake pads/tailpipes of cars. This profile was also dominated by Ni and V; both are widely known to be released by the combustion of heavy engine oil [*Police et al.*, 2016; *Vallius et al.*, 2005]. The V and Ni in this context were mainly released by shipping emissions, refining of crude oil and industrial power plants using heavy oil [*Minguillón et al.*, 2014].

3.5.1.4. Factor 4: Coal-Fired Combustion

The dominant presence of As, Bi, OC, and OP can be classified as a coal-fired combustion source. The EV for As, Bi, OC, and OP to this factor was 66%, 68%, 50%, and 46%, respectively. As is the major species released into atmosphere from coal-fired power plants [*Khan et al.*, 2016a; *Meij and te Winkel*, 2007; *Moreno et al.*, 2013; *Querol et al.*, 1995], there are several coal-fired power plants installed on the west coast of Malaysia. During the southwest monsoon season, the synoptic wind will predominantly blow from the southwest direction. Thus, the nearby power plants may well influence the emission of As, along with other low-concentration marker species. The ratio of OC/EC to this factor is 7.3, which is higher compared to the background minimum ratio of 0.55, as reported in the previous section. The value is also higher compared to 5.6, 2.97, and 2.70 for coal combustion, coal-fired boilers, and the residential coal burning source, as reported by *Huang et al.* [2006], *Watson et al.* [2001], and *Zhang et al.* [2009], respectively. However, it is still low compared to the value of 12.0 for the OC/EC ratio representing the coal combustion source as reported by *Cao et al.* [2003]. With an overall account of 25% of the estimated $PM_{2.5}$ concentrations, this factor is the largest contributor to $PM_{2.5}$ at the site during the southwest monsoon season with a dominant influence in the fourth week of June 2014.

3.5.1.5. Factor 5: Mineral Dust

This factor profile was enriched predominantly by the Mg^{2+} (70% of EV) followed by the small EVs of Na^+, Ba, Cu, and K^+ at 19%, 14%, 12%, and 11%, respectively. Mg^{2+} can be resuspended into ambient air from mineral dust sources. Mineral dust contributed 8% of the estimated $PM_{2.5}$ concentrations. This source was pronounced in the week 1 of 2014, as demonstrated in Figure 8c.

Figure 8. (a) A correlation of the estimated $PM_{2.5}$ by PMF 5.0 and observed $PM_{2.5}$ (HVS), (b) contribution of each source by the percentage (UD: undefined), and (c) time series of the source-specific mass concentration of $PM_{2.5}$ prediction by PMF version 5.0.

3.5.1.6. Factor 6: SIA Coupled With F^-

The SIA was characterized by NH_4^+, F^-, and SO_4^{2-}. Strong solar radiation during the dry season may trigger the oxidation of SO_2 to SO_4^{2-}, as observed by *Querol et al.* [1999] during the summer season. nss-SO_4^{2-} was estimated at 1.95 µg m^{-3} (98% of the total SO_4^{2-}), suggesting that the dominant source of sulfate and its precursors originated from anthropogenic sources. Anthropogenic SO_2 is predominantly released from the point sources [*Heo et al.*, 2009], where industrial combustion plays a vital role in the release of SO_2 into ambient air. NH_4^+ is formed in the atmosphere from the precursor gas NH_3. Meanwhile, *Police et al.* [2016] reported that the airborne F^- is mostly emitted in gaseous form and released from anthropogenic sources. However, F^- was detected in $PM_{2.5}$ particulate form, and this might be due to the phenomenon of gas-to-particle conversion. Several researchers have reported SIA in $PM_{2.5}$ in Beijing [*Zhang et al.*, 2013], Lisbon [*Almeida et al.*, 2005], New Taipei City [*Gugamsetty et al.*, 2012], and northern Vietnam [*Hang and Kim Oanh*, 2014]. Overall, this factor accounts for 15% of the $PM_{2.5}$ estimated concentrations and showed a dominant presence during early September 2014 (Figure 8c) with the highest contribution on 28 August 2014.

3.5.1.7. Factor 7: Motor Vehicle Emissions Coupled With Sea Salt [II]

The motor vehicle emission source was characterized by the presence of Fe, Mn, Mg, EC, OC, OP, Na^+, and Cl^-. The compositions of this factor profile are significant signatories to both traffic combustion and noncombustion sources. EC and OC are widely used as markers of motor vehicles [*Amato et al.*, 2014; *Khan et al.*, 2010a, 2010c; *Song et al.*, 2006]. EC might be released into ambient air as result of the incomplete combustion of fossil fuel. The EC/OC ratio value was 0.51 (0.09–1.82), which was much higher than the 0.03 ratio value obtained for biomass burning [*Chen et al.*, 2011]. Based on sampling site background, the emissions of EC and OC in this study were comparatively similar to the emission factors for diesel and gasoline as calculated in Minnesota, USA [*Chen et al.*, 2011]. Thus, the combustion of gasoline and diesel were both found to contribute to this factor profile. The OC/EC ratio (to this factor) was 0.85, which is comparable to the values of 0.88 and 1.1, as reported by *Watson et al.* [2001] and *Zhang et al.* [2009], respectively, for vehicular combustion sources. Thus, it is notable that the ratio of OC/EC obtained in this study is similar to the ratio for the motor vehicle source obtained from other studies. The ratio of OC/EC is also comparable to the 0.55 background minimum ratio of OC/EC, reported in the previous section. Hence, the ratio of OC/EC strongly supports that this factor profile represents the background emissions from motor vehicle combustion, i.e., local transportation. Further, the concentration and pattern of CO (as described in the previous section) represent a proxy for emissions from motor vehicles. As shown in Figure S12, the covariation of CO showed that the assignment of combustion factor is consistent with the elevated concentrations of CO. Meanwhile, the presence of Fe and Mn was predominantly determined as being derived from non-combustion origins. This factor profile was also dominated by Na^+ and Cl^- with 21% and 32% of EV, respectively, which supports the influence of marine aerosol. Overall, this factor is the second largest contributor to the $PM_{2.5}$ at the site during the dry season with 24% (of the estimated $PM_{2.5}$) and demonstrated a pronounced concentration in July and September 2014.

3.6. Transboundary Impact From SEA and Tracing the Source Regions

Figure 9 shows the distribution of the PSCF value of the $PM_{2.5}$ sources identified by PMF 5.0. The days with the highest concentrations of $PM_{2.5}$ contributing to factor 1 to 7 were selected. The 48 h BTs for the selected days were then calculated and compared to the total integrated BT for the sampling period. The PSCF results showed that the region with a high probability of being the origin of factor 1 is the North Sumatra area with an influence of air mass originating from the ocean. Also, high numbers of hotspots are located in the Sumatra region during the dry southwest monsoon. A strong fire intensity was also observed in the above region representing a strong magnitude of fire counts. As shown in Figure 2a, these satellite-detected fire counts are not only confined to the burning of agricultural waste and forest fires but also the smoke emitted from the spontaneous smoldering combustion of peat soil. The combined effect of the two fire sources serves to magnify the aerosol pollution during the dry southwest monsoon in Malaysia and its neighboring countries. It is presumed that there is a greater accumulating effect on $PM_{2.5}$ as it can be transported to intercontinent locations. El Niño is most likely to play major role behind this as it predominantly brings dry weather to SEA, as suggested by *Satterfield* [2015]. This dry weather usually makes the overall situation of aerosol pollution far worse. Overall, Figure 1a demonstrates that the emission of $PM_{2.5}$ per year was significantly higher in Jakarta, the capital city of Indonesia. The BLH on the trajectories, as well as the gridded region, showed that the concentration of aerosol at the sampling site and in South Sumatra was largely concentrated in the
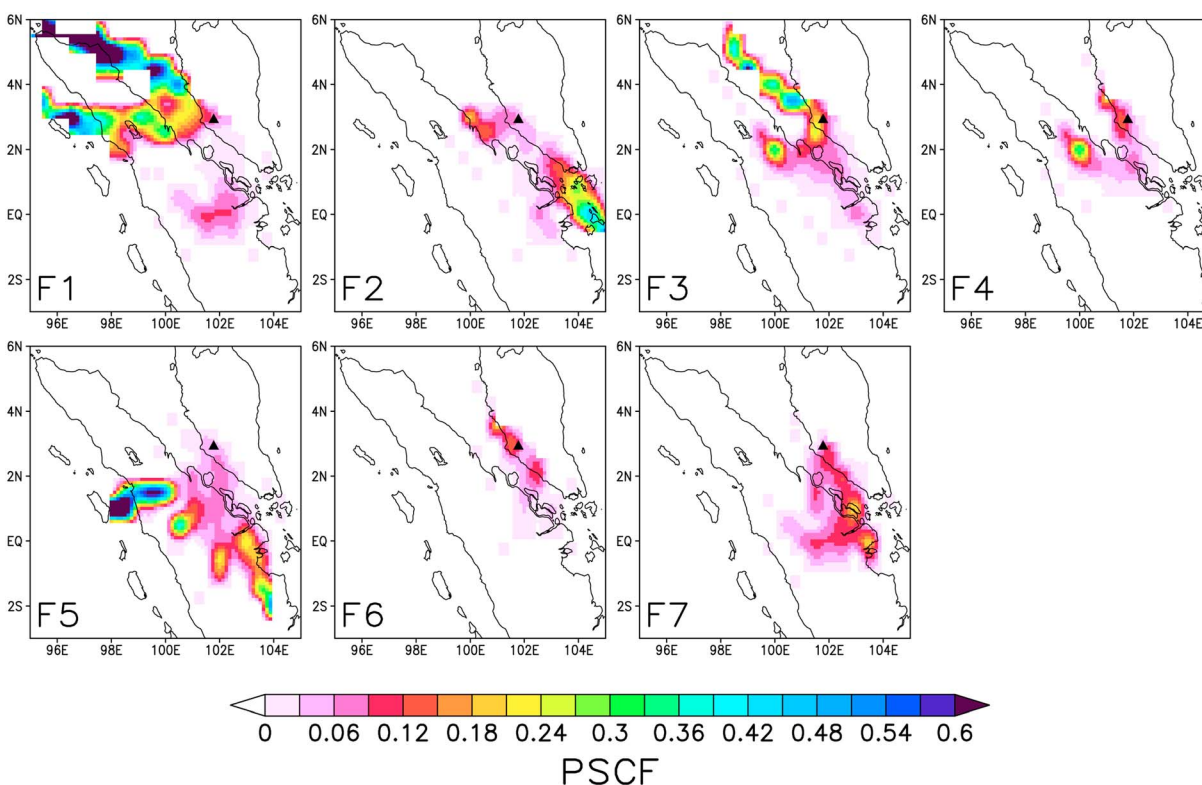
Figure 9. PSCF modeled for each of the PM$_{2.5}$ source prediction by PMF version 5.0. The symbol of triangle represents the sampling station.

comparatively thick BLH. Factor 2 was seen to be influenced by the air mass transporting from the ocean. Factors 3 and 4 were governed by the Malacca Strait. Factor 3 was influenced by a local factor as well as the air masses from the Malacca Strait. The local factor was either combustion of heavy oil in shipping activities and/or several power plants along the coast of the Malacca Straits, which uses heavy oil to produce electricity. As for factor 4, the presence of petroleum refineries and coal-fired power plants on the west coast of Malaysia is likely to be the reason. The air mass travelling from South Sumatra might carry the mineral dust and that is a potential contributor to factor 5. The sources of factor 6 were found in the local area. As for factor 7, the sources were mainly influenced by both local and transboundary areas.

4. Conclusions

This study focused on the physicochemical properties of aerosols and the combined measurements of in situ and gravimetric mass, satellite data, and SA techniques. During the southwest monsoon, the transport of air masses originating or passing over the islands of Sumatra and Kalimantan region, areas with the largest number of biomass burning or wildfire hotspots, potentially impacted on the severe haze episodes in Malaysia. The air mass transports from the downwind region and the prevalence of lower mixing depths and low atmospheric pressure govern the concentration of PM$_{2.5}$ at this study area. The results showed that the range of 24 h average concentrations of PM$_{2.5}$ was 6.64 µg m^{-3} to 68.2 µg m^{-3}. The predominant ions and trace species were found to be NH$_4^+$, K$^+$, Ca^{2+}, Na$^+$, Zn, Al, Mg, and Fe. The results of SOC estimation, by applying the minimum ratio of OC to EC (0.55), showed that the largest fraction of total OC was SOC, and the remaining OC may have been released from primary combustion sources. Furthermore, the appearance of haze was clearly observed on 24–30 June 2014, with a high OP/OC4 value (>4). The results of the correlation analysis between nss-K$^+$ and EC indicated that EC tends to be emitted from the biomass burning-prone areas. Seven sources were identified by the PMF SA technique. The contribution of the seven factors follows the trend coal-fired combustion > motor vehicle emissions coupled with sea salt [II] > SIA coupled with the F$^-$ > mineral dust > biomass burning coupled with sea salt [I], road dust and fuel oil combustion > aged sea salt and mixed industrial emissions. The results of the PSCF and the HYSPLIT model suggest that the

outline of source regions were consistent to the predicted sources by PMF 5.0. The PSCF successfully reproduced the impact of biomass burning from Sumatra, maritime sea salt, local activities, point sources at the west coast of Peninsular Malaysia, and the emission of traffic from local and transboundary areas that were clearly affecting the concentration of $PM_{2.5}$ in a tropical site during the summer monsoon.

References

Almeida, S. M., C. A. Pio, M. C. Freitas, M. A. Reis, and M. A. Trancoso (2005), Source apportionment of fine and coarse particulate matter in a sub-urban area at the Western European Coast, *Atmos. Environ.*, *39*(17), 3127–3138, doi:10.1016/j.atmosenv.2005.01.048.

Amato, F., et al. (2011), Size and time-resolved roadside enrichment of atmospheric particulate pollutants, *Atmos. Chem. Phys.*, *11*(6), 2917–2931, doi:10.5194/acp-11-2917-2011.

Amato, F., I. Rivas, M. Viana, T. Moreno, L. Bouso, C. Reche, M. Àlvarez-Pedrerol, A. Alastuey, J. Sunyer, and X. Querol (2014), Sources of indoor and outdoor $PM_{2.5}$ concentrations in primary schools, *Sci. Total Environ.*, *490*, 757–765, doi:10.1016/j.scitotenv.2014.05.051.

Amil, N., M. T. Latif, M. F. Khan, and M. Mohamad (2016), Seasonal variability of $PM_{2.5}$ composition and sources in the Klang Valley urban-industrial environment, *Atmos. Chem. Phys.*, *16*(8), 5357–5381, doi:10.5194/acp-16-5357-2016.

Ashbaugh, L. L., W. C. Malm, and W. Z. Sadeh (1985), A residence time probability analysis of sulfur concentrations at grand Canyon National Park, *Atmos. Environ.*, *19*(8), 1263–1270, doi:10.1016/0004-6981(85)90256-2.

Baumann, K., R. K. M. Jayanty, and J. B. Flanagan (2008), Fine particulate matter source apportionment for the chemical speciation trends network site at Birmingham, Alabama, using positive matrix factorization, *J. Air Waste Manage. Assoc.*, *58*(1), 27–44, doi:10.3155/1047-3289.58.1.27.

Beddows, D. C. S., R. M. Harrison, D. C. Green, and G. W. Fuller (2015), Receptor modelling of both particle composition and size distribution from a background site in London, UK, *Atmos. Chem. Phys.*, *15*(17), 10,107–10,125, doi:10.5194/acp-15-10107-2015.

Begum, B. A., E. Kim, C.-H. Jeong, D.-W. Lee, and P. K. Hopke (2005), Evaluation of the potential source contribution function using the 2002 Quebec forest fire episode, *Atmos. Environ.*, *39*(20), 3719–3724, doi:10.1016/j.atmosenv.2005.03.008.

Brown, S. G., S. Eberly, P. Paatero, and G. A. Norris (2015), Methods for estimating uncertainty in PMF solutions: Examples with ambient air and water quality data and guidance on reporting PMF results, *Sci. Total Environ.*, *518–519*, 626–635.

Cachier, H., M.-P. Bremond, and P. Buat-MÉNard (1989), Determination of atmospheric soot carbon with a simple thermal method, *Tellus B*, *41B*(3), 379–390, doi:10.1111/j.1600-0889.1989.tb00316.x.

Callén, M. S., A. Iturmendi, and J. M. López (2014), Source apportionment of atmospheric $PM_{2.5}$-bound polycyclic aromatic hydrocarbons by a PMF receptor model. Assessment of potential risk for human health, *Environ. Pollut.*, *195*, 167–177, doi:10.1016/j.envpol.2014.08.025.

Cao, J. J., S. C. Lee, K. F. Ho, X. Y. Zhang, S. C. Zou, K. Fung, J. C. Chow, and J. G. Watson (2003), Characteristics of carbonaceous aerosol in Pearl River Delta region, China during 2001 winter period, *Atmos. Environ.*, *37*(11), 1451–1460, doi:10.1016/S1352-2310(02)01002-6.

Carvalho, A., C. Pio, C. Santos, and C. Alves (2006), Particulate carbon in the atmosphere of a Finnish forest and a German anthropogenically influenced grassland, *Atmos. Res.*, *80*(2–3), 133–150, doi:10.1016/j.atmosres.2005.07.001.

Castro, L. M., C. A. Pio, R. M. Harrison, and D. J. T. Smith (1999), Carbonaceous aerosol in urban and rural European atmospheres: Estimation of secondary organic carbon concentrations, *Atmos. Environ.*, *33*(17), 2771–2781, doi:10.1016/S1352-2310(98)00331-8.

Chang, D., and Y. Song (2010), Estimates of biomass burning emissions in tropical Asia based on satellite-derived data, *Atmos. Chem. Phys.*, *10*(5), 2335–2351, doi:10.5194/acp-10-2335-2010.

Chen, L. W. A., J. G. Watson, J. C. Chow, D. W. DuBois, and L. Herschberger (2011), $PM_{2.5}$ source apportionment: Reconciling receptor models for U.S. nonurban and urban long-term networks, *J. Air Waste Manage. Assoc.*, *61*(11), 1204–1217, doi:10.1080/10473289.2011.619082.

Cheng, Y., K.-B. He, F.-K. Duan, M. Zheng, Z.-Y. Du, Y.-L. Ma, and J.-H. Tan (2011), Ambient organic carbon to elemental carbon ratios: Influences of the measurement methods and implications, *Atmos. Environ.*, *45*(12), 2060–2066, doi:10.1016/j.atmosenv.2011.01.064.

Cheng, Y., K.-B. He, F.-K. Duan, Z.-Y. Du, M. Zheng, and Y.-L. Ma (2014), Ambient organic carbon to elemental carbon ratios: Influence of the thermal–optical temperature protocol and implications, *Sci. Total Environ.*, *468–469*, 1103–1111, doi:10.1016/j.scitotenv.2013.08.084.

Choi, J.-K., J.-B. Heo, S.-J. Ban, S.-M. Yi, and K.-D. Zoh (2013), Source apportionment of $PM_{2.5}$ at the coastal area in Korea, *Sci. Total Environ.*, *447*, 370–380, doi:10.1016/j.scitotenv.2012.12.047.

Chong, C., W. Ni, L. Ma, P. Liu, and Z. Li (2015), The use of energy in Malaysia: Tracing energy flows from primary source to end use, *Energies*, *8*(4), 2828–2866.

Cong, Z., S. Kang, K. Kawamura, B. Liu, X. Wan, Z. Wang, S. Gao, and P. Fu (2015), Carbonaceous aerosols on the south edge of the Tibetan Plateau: Concentrations, seasonality and sources, *Atmos. Chem. Phys.*, *15*(3), 1573–1584, doi:10.5194/acp-15-1573-2015.

Crutzen, P. J., and M. O. Andreae (1990), Biomass burning in the tropics: Impact on atmospheric chemistry and biogeochemical cycles, *Science*, *250*(4988), 1669–1678.

Dai, W., J. Gao, G. Cao, and F. Ouyang (2013), Chemical composition and source identification of $PM_{2.5}$ in the suburb of Shenzhen, China, *Atmos. Res.*, *122*, 391–400, doi:10.1016/j.atmosres.2012.12.004.

Dall'Osto, M., X. Querol, F. Amato, A. Karanasiou, F. Lucarelli, S. Nava, G. Calzolai, and M. Chiari (2013), Hourly elemental concentrations in $PM_{2.5}$ aerosols sampled simultaneously at urban background and road site during SAPUSS—Diurnal variations and PMF receptor modelling, *Atmos. Chem. Phys.*, *13*(8), 4375–4392, doi:10.5194/acp-13-4375-2013.

Duan, J., J. Tan, D. Cheng, X. Bi, W. Deng, G. Sheng, J. Fu, and M. H. Wong (2007), Sources and characteristics of carbonaceous aerosol in two largest cities in Pearl River Delta region, China, *Atmos. Environ.*, *41*(14), 2895–2903, doi:10.1016/j.atmosenv.2006.12.017.

Duarte, R. M. B. O., C. L. Mieiro, A. Penetra, C. A. Pio, and A. C. Duarte (2008), Carbonaceous materials in size-segregated atmospheric aerosols from urban and coastal-rural areas at the Western European Coast, *Atmos. Res.*, *90*(2–4), 253–263, doi:10.1016/j.atmosres.2008.03.003.

Fang, T., H. Guo, V. Verma, R. E. Peltier, and R. J. Weber (2015), $PM_{2.5}$ water-soluble elements in the southeastern United States: Automated analytical method development, spatiotemporal distributions, source apportionment, and implications for heath studies, *Atmos. Chem. Phys.*, *15*(20), 11,667–11,682.

Forsyth, T. (2014), Public concerns about transboundary haze: A comparison of Indonesia, Singapore, and Malaysia, *Global Environ. Change*, *25*, 76–86, doi:10.1016/j.gloenvcha.2014.01.013.

Fujii, Y., W. Iriana, M. Oda, A. Puriwigati, S. Tohno, P. Lestari, A. Mizohata, and H. S. Huboyo (2014), Characteristics of carbonaceous aerosols emitted from peatland fire in Riau, Sumatra, Indonesia, *Atmos. Environ.*, *87*, 164–169, doi:10.1016/j.atmosenv.2014.01.037.

Fujii, Y., M. Mahmud, M. Oda, S. Tohno, J. Matsumoto, and A. Mizohata (2016), A key indicator of transboundary particulate matter pollution derived from Indonesian peatland fires in Malaysia, *Aerosol Air Qual. Res.*, *16*, 69–78, doi:10.4209/aaqr.2015.04.0215.

Grimm, H., and D. J. Eatough (2009), Aerosol measurement: The use of optical light scattering for the determination of particulate size distribution, and particulate mass, including the semi-volatile fraction, *J. Air Waste Manage. Assoc.*, *59*(1), 101–107, doi:10.3155/1047-3289.59.1.101.

Gugamsetty, B., H. Wei, C.-N. Liu, A. Awasthi, S.-C. Hsu, C.-J. Tsai, G.-D. Roam, Y.-C. Wu, and C.-F. Chen (2012), Source characterization and apportionment of PM_{10}, $PM_{2.5}$ and $PM_{0.1}$ by using positive matrix factorization, *Aerosol Air Qual. Res*, *12*, 476–491.

Hang, N. T., and N. T. Kim Oanh (2014), Chemical characterization and sources apportionment of fine particulate pollution in a mining town of Vietnam, *Atmos. Res.*, *145–146*, 214–225, doi:10.1016/j.atmosres.2014.04.009.

Harrison, R. M., and J. Yin (2008), Sources and processes affecting carbonaceous aerosol in central England, *Atmos. Environ.*, *42*(7), 1413–1423, doi:10.1016/j.atmosenv.2007.11.004.

Harrison, R. M., D. C. S. Beddows, and M. Dall'Osto (2011), PMF analysis of wide-range particle size spectra collected on a major highway, *Environ. Sci. Technol.*, *45*(13), 5522–5528, doi:10.1021/es2006622.

Hasheminassab, S., N. Daher, A. Saffari, D. Wang, B. D. Ostro, and C. Sioutas (2014), Spatial and temporal variability of sources of ambient fine particulate matter ($PM_{2.5}$) in California, *Atmos. Chem. Phys.*, *14*(22), 12,085–12,097, doi:10.5194/acp-14-12085-2014.

Hedberg, E., L. Gidhagen, and C. Johansson (2005), Source contributions to PM_{10} and arsenic concentrations in central Chile using positive matrix factorization, *Atmos. Environ.*, *39*(3), 549–561, doi:10.1016/j.atmosenv.2004.11.001.

Heil, A., and J. Goldammer (2001), Smoke-haze pollution: A review of the 1997 episode in Southeast Asia, *Reg. Environ. Change*, *2*(1), 24–37, doi:10.1007/s101130100021.

Heil, A., B. Langmann, and E. Aldrian (2007), Indonesian peat and vegetation fire emissions: Study on factors influencing large-scale smoke haze pollution using a regional atmospheric chemistry model, *Mitigation Adapt. Strategies Global Change*, *12*(1), 113–133, doi:10.1007/s11027-006-9045-6.

Henry, R. C. (1987), Current factor analysis receptor models are ill-posed, *Atmos. Environ.*, *21*(8), 1815–1820, doi:10.1016/0004-6981(87)90122-3.

Heo, J. B., P. K. Hopke, and S. M. Yi (2009), Source apportionment of $PM_{2.5}$ in Seoul, Korea, *Atmos. Chem. Phys.*, *9*(14), 4957–4971, doi:10.5194/acp-9-4957-2009.

Hopke, P. K. (2003), The evolution of chemometrics, *Anal.Chim. Acta*, *500*(1–2), 365–377, doi:10.1016/S0003-2670(03)00944-9.

Hopke, P. K., L. A. Barrie, S. M. Li, M. D. Cheng, C. Li, and Y. Xie (1995), Possible sources and preferred pathways for biogenic and non-sea-salt sulfur for the high Arctic, *J. Geophys. Res.*, *100*, 16,595–16,603, doi:10.1029/95JD01712.

Huang, L., J. R. Brook, W. Zhang, S. M. Li, L. Graham, D. Ernst, A. Chivulescu, and G. Lu (2006), Stable isotope measurements of carbon fractions (OC/EC) in airborne particulate: A new dimension for source characterization and apportionment, *Atmos. Environ.*, *40*(15), 2690–2705, doi:10.1016/j.atmosenv.2005.11.062.

Huang, X. H., Q. Bian, W. M. Ng, P. K. Louie, and J. Z. Yu (2014), Characterization of $PM_{2.5}$ major components and source investigation in suburban Hong Kong: A one year monitoring study, *Aerosol Air Qual. Res.*, *14*(1), 237–250.

IOM (2006), *Comparing Estimated Risks for Air Pollution with Risks for Other Health Effects*, Institute of Occupational Medicine, Edinburgh, U. K.

Jamhari, A. A., M. Sahani, M. T. Latif, K. M. Chan, H. S. Tan, M. F. Khan, and N. Mohd Tahir (2014), Concentration and source identification of polycyclic aromatic hydrocarbons (PAHs) in PM_{10} of urban, industrial and semi-urban areas in Malaysia, *Atmos. Environ.*, *86*, 16–27, doi:10.1016/j.atmosenv.2013.12.019.

Juneng, L., M. T. Latif, F. T. Tangang, and H. Mansor (2009), Spatio-temporal characteristics of PM_{10} concentration across Malaysia, *Atmos. Environ.*, *43*(30), 4584–4594, doi:10.1016/j.atmosenv.2009.06.018.

Juneng, L., M. T. Latif, and F. Tangang (2011), Factors influencing the variations of PM_{10} aerosol dust in Klang Valley, Malaysia during the summer, *Atmos. Environ.*, *45*(26), 4370–4378, doi:10.1016/j.atmosenv.2011.05.045.

Keywood, M. D., G. P. Ayers, J. L. Gras, R. Boers, and C. P. Leong (2003), Haze in the Klang Valley of Malaysia, *Atmos. Chem. Phys.*, *3*(3), 591–605, doi:10.5194/acp-3-591-2003.

Khan, M. F., K. Hirano, and S. Masunaga (2010a), Quantifying the sources of hazardous elements of suspended particulate matter aerosol collected in Yokohama, Japan, *Atmos. Environ.*, *44*(21), 2646–2657.

Khan, M. F., Y. Shirasuna, K. Hirano, and S. Masunaga (2010b), Characterization of $PM_{2.5}$, $PM_{2.5-10}$ and $PM_{>10}$ in ambient air, Yokohama, Japan, *Atmos. Res.*, *96*(1), 159–172, doi:10.1016/j.atmosres.2009.12.009.

Khan, M. F., Y. Shirasuna, K. Hirano, and S. Masunaga (2010c), Urban and suburban aerosol in Yokohama, Japan: A comprehensive chemical characterization, *Environ. Monit. Assess.*, *171*(1–4), 441–456, doi:10.1007/s10661-009-1290-1.

Khan, M. F., K. Hirano, and S. Masunaga (2012), Assessment of the sources of suspended particulate matter aerosol using US EPA PMF 3.0, *Environ. Monit. Assess.*, *184*(2), 1063–1083, doi:10.1007/s10661-011-2021-y.

Khan, M. F., M. T. Latif, N. Amil, L. Juneng, N. Mohamad, M. S. M. Nadzir, and H. M. S. Hoque (2015a), Characterization and source apportionment of particle number concentration at a semi-urban tropical environment, *Environ. Sci. Pollut. Res.*, *22*, 13,111–13,13126.

Khan, M. F., M. T. Latif, L. Juneng, N. Amil, M. S. Mohd Nadzir, and H. M. Syedul Hoque (2015b), Physicochemical factors and sources of particulate matter at residential urban environment in Kuala Lumpur, *J. Air Waste Manage. Assoc.*, *65*(8), 958–969, doi:10.1080/10962247.2015.1042094.

Khan, M. F., M. T. Latif, C. H. Lim, N. Amil, S. A. Jaafar, D. Dominick, M. S. Mohd Nadzir, M. Sahani, and N. M. Tahir (2015c), Seasonal effect and source apportionment of polycyclic aromatic hydrocarbons in $PM_{2.5}$, *Atmos. Environ.*, *106*, 178–190, doi:10.1016/j.atmosenv.2015.01.077.

Khan, M. F., M. T. Latif, W. H. Saw, N. Amil, M. S. M. Nadzir, M. Sahani, N. M. Tahir, and J. X. Chung (2016a), Fine particulate matter in the tropical environment: Monsoonal effects, source apportionment, and health risk assessment, *Atmos. Chem. Phys.*, *16*(2), 597–617, doi:10.5194/acp-16-597-2016.

Khan, M. M., K. Zaman, D. Irfan, U. Awan, G. Ali, P. Kyophilavong, M. Shahbaz, and I. Naseem (2016b), Triangular relationship among energy consumption, air pollution and water resources in Pakistan, *J. Cleaner Prod.*, *112*(Part 2), 1375–1385, doi:10.1016/j.jclepro.2015.01.094.

Kim, E., and P. K. Hopke (2004), Comparison between conditional probability function and nonparametric regression for fine particle source directions, *Atmos. Environ.*, *38*(28), 4667–4673, doi:10.1016/j.atmosenv.2004.05.035.

Kim, E., and P. K. Hopke (2007), Source characterization of ambient fine particles in the Los Angeles basin, *J. Environ. Eng. Sci.*, *6*(4), 343–353, doi:10.1139/s06-054.

Kim Oanh, N. T., et al. (2006), Particulate air pollution in six Asian cities: Spatial and temporal distributions, and associated sources, *Atmos. Environ.*, *40*(18), 3367–3380, doi:10.1016/j.atmosenv.2006.01.050.

Kondo, Y., L. Sahu, N. Moteki, F. Khan, N. Takegawa, X. Liu, M. Koike, and T. Miyakawa (2011), Consistency and traceability of black carbon measurements made by laser-induced incandescence, thermal-optical transmittance, and filter-based photo-absorption techniques, *Aerosol Sci. Technol.*, *45*(2), 295–312, doi:10.1080/02786826.2010.533215.

Latif, M. T., D. Dominick, F. Ahamad, M. F. Khan, L. Juneng, F. M. Hamzah, and M. S. Nadzir (2014), Long term assessment of air quality from a background station on the Malaysian Peninsula, *Sci. Total Environ.*, *482–483*, 336–348, doi:10.1016/j.scitotenv.2014.02.132.

Lestari, P., and Y. D. Mauliadi (2009), Source apportionment of particulate matter at urban mixed site in Indonesia using PMF, *Atmos. Environ.*, *43*(10), 1760–1770, doi:10.1016/j.atmosenv.2008.12.044.

Levine, J. S. (1999), The 1997 fires in Kalimantan and Sumatra, Indonesia: Gaseous and particulate emissions, *Geophys. Res. Lett.*, *26*, 815–818, doi:10.1029/1999GL900067.

Lonati, G., M. Giugliano, and S. Ozgen (2008), Primary and secondary components of $PM_{2.5}$ in Milan (Italy), *Environ. Int.*, *34*(5), 665–670, doi:10.1016/j.envint.2007.12.009.

Malm, W. C., C. E. Johnson, and J. F. Bresch (1986), in *Application of Principal Component Analysis for Purposes of Identifying Source-Receptor Relationships*, edited by T. G. Pace, pp. 127–148, Air Pollution Control Association, Pittsburgh, Pa.

Malm, W. C., J. F. Sisler, D. Huffman, R. A. Eldred, and T. A. Cahill (1994), Spatial and seasonal trends in particle concentration and optical extinction in the United States, *J. Geophys. Res.*, *99*, 1347–1347, doi:10.1029/93JD02916.

Mancilla, Y., A. Mendoza, M. P. Fraser, and P. Herckes (2015), Chemical characterization of fine organic aerosol for source apportionment at Monterrey, Mexico, *Atmos. Chem. Phys. Discuss.*, *15*(13), 17,967–18,010, doi:10.5194/acpd-15-17967-2015.

Meij, R., and H. te Winkel (2007), The emissions of heavy metals and persistent organic pollutants from modern coal-fired power stations, *Atmos. Environ.*, *41*(40), 9262–9272, doi:10.1016/j.atmosenv.2007.04.042.

Minguillón, M. C., M. Cirach, G. Hoek, B. Brunekreef, M. Tsai, K. de Hoogh, A. Jedynska, I. M. Kooter, M. Nieuwenhuijsen, and X. Querol (2014), Spatial variability of trace elements and sources for improved exposure assessment in Barcelona, *Atmos. Environ.*, *89*, 268–281, doi:10.1016/j.atmosenv.2014.02.047.

Miyazaki, Y., Y. Kondo, S. Han, M. Koike, D. Kodama, Y. Komazaki, H. Tanimoto, and H. Matsueda (2007), Chemical characteristics of water-soluble organic carbon in the Asian outflow, *J. Geophys. Res.*, *112*, D22S30, doi:10.1029/2007JD009116.

Mohd Tahir, N., S. Suratman, F. T. Fong, M. S. Hamzah, and M. T. Latif (2013), Temporal distribution and chemical characterization of atmospheric particulate matter in the eastern coast of Peninsular Malaysia, *Aerosol Air Qual. Res.*, *13*(2), 584–595, doi:10.4209/aaqr.2012.08.0216.

Moreno, T., et al. (2013), Daily and hourly sourcing of metallic and mineral dust in urban air contaminated by traffic and coal-burning emissions, *Atmos. Environ.*, *68*, 33–44, doi:10.1016/j.atmosenv.2012.11.037.

Mustaffa, N. I. H., M. T. Latif, M. M. Ali, and M. F. Khan (2014), Source apportionment of surfactants in marine aerosols at different locations along the Malacca Straits, *Environ. Sci. Pollut. Res.*, *21*(10), 6590–6602.

Norris, G., R. Duvall, S. Brown, and S. Bai (2014), EPA positive matrix factorization (PMF) 5.0 fundamentals & user guide, Prepared for the U.S. Environmental Protection Agency, Washington, D. C., by the National Exposure Research Laboratory, Research Triangle Park.

Novakov, T., M. O. Andreae, R. Gabriel, T. W. Kirchstetter, O. L. Mayol-Bracero, and V. Ramanathan (2000), Origin of carbonaceous aerosols over the tropical Indian Ocean: Biomass burning or fossil fuels?, *Geophys. Res. Lett.*, *27*, 4061–4064, doi:10.1029/2000GL011759.

Ogulei, D., P. K. Hopke, and L. A. Wallace (2006a), Analysis of indoor particle size distributions in an occupied townhouse using positive matrix factorization, *Indoor Air*, *16*(3), 204–215, doi:10.1111/j.1600-0668.2006.00418.x.

Ogulei, D., P. K. Hopke, L. Zhou, P. J. Patrick, N. Nair, and J. M. Ondov (2006b), Source apportionment of Baltimore aerosol from combined size distribution and chemical composition data, *Atmos. Environ.*, *40*(Supplement 2), 396–410, doi:10.1016/j.atmosenv.2005.11.075.

Othman, J., M. Sahani, M. Mahmud, and M. K. Sheikh Ahmad (2014), Transboundary smoke haze pollution in Malaysia: Inpatient health impacts and economic valuation, *Environ. Pollut.*, *189*, 194–201, doi:10.1016/j.envpol.2014.03.010.

Paatero, P. (1997), Least squares formulation of robust non-negative factor analysis, *Chemom. Intell. Lab. Syst.*, *37*(1), 23–35, doi:10.1016/S0169-7439(96)00044-5.

Paatero, P., and U. Tapper (1994), Positive matrix factorization: A non-negative factor model with optimal utilization of error estimates of data values, *Environmetrics*, *5*(2), 111–126, doi:10.1002/env.3170050203.

Paatero, P., S. Eberly, S. G. Brown, and G. A. Norris (2014), Methods for estimating uncertainty in factor analytic solutions, *Atmos. Meas. Tech.*, *7*, 781–797.

Page, S. E., F. Siegert, J. O. Rieley, H.-D. V. Boehm, A. Jaya, and S. Limin (2002), The amount of carbon released from peat and forest fires in Indonesia during 1997, *Nature*, *420*(6911), 61–65.

Pio, C., M. Cerqueira, R. M. Harrison, T. Nunes, F. Mirante, C. Alves, C. Oliveira, A. Sanchez de la Campa, B. Artíñano, and M. Matos (2011), OC/EC ratio observations in Europe: Re-thinking the approach for apportionment between primary and secondary organic carbon, *Atmos. Environ.*, *45*(34), 6121–6132, doi:10.1016/j.atmosenv.2011.08.045.

Police, S., S. K. Sahu, and G. G. Pandit (2016), Chemical characterization of atmospheric particulate matter and their source apportionment at an emerging industrial coastal city, Visakhapatnam, India, *Atmos. Pollut. Res.*, *7*(4), 725–733, doi:10.1016/j.apr.2016.03.007.

Polissar, A. V., P. K. Hopke, W. C. Malm, and J. F. Sisler (1998a), Atmospheric aerosol over Alaska: 1. Spatial and seasonal variability, *J. Geophys. Res.*, *103*, 19,035–19,044, doi:10.1029/98JD01365.

Polissar, A. V., P. K. Hopke, P. Paatero, W. C. Malm, and J. F. Sisler (1998b), Atmospheric aerosol over Alaska: 2. Elemental composition and sources, *J. Geophys. Res.*, *103*, 19,045–19,057, doi:10.1029/98JD01212.

Pope, C. A., M. Ezzati, and D. W. Dockery (2009), Fine-particulate air pollution and life expectancy in the United States, *N. Engl. J. Med.*, *360*(4), 376–386, doi:10.1056/NEJMsa0805646.

Querol, X., J. Fernández-Turiel, and A. López-Soler (1995), Trace elements in coal and their behaviour during combustion in a large power station, *Fuel*, *74*(3), 331–343, doi:10.1016/0016-2361(95)93464-O.

Querol, X., A. Alastuey, A. Lopez-Soler, F. Plana, J. A. Puicercus, E. Mantilla, and J. L. Palau (1999), Daily evolution of sulphate aerosols in a rural area, northeastern Spain—Elucidation of an atmospheric reservoir effect, *Environ. Pollut.*, *105*(3), 397–407, doi:10.1016/S0269-7491(99)00037-8.

Rahman, S. A., M. S. Hamzah, A. K. Wood, M. S. Elias, N. Ashifa, and E. Sanuri (2011), Sources apportionment of fine and coarse aerosol in Klang Valley, Kuala Lumpur using positive matrix factorization, *Atmos. Pollut. Res.*, *2*(2), 197–206, doi:10.5094/APR.2011.025.

Ramadan, Z., X.-H. Song, and P. K. Hopke (2000), Identification of sources of phoenix aerosol by positive matrix factorization, *J. Air Waste Manage. Assoc.*, *50*(8), 1308–1320, doi:10.1080/10473289.2000.10464173.

Reid, J. S., et al. (2013), Observing and understanding the Southeast Asian aerosol system by remote sensing: An initial review and analysis for the Seven Southeast Asian Studies (7SEAS) program, *Atmos. Res.*, *122*, 403–468, doi:10.1016/j.atmosres.2012.06.005.

Remoundaki, E., P. Kassomenos, E. Mantas, N. Mihalopoulos, and M. Tsezos (2013), Composition and mass closure of $PM_{2.5}$ in urban environment (Athens, Greece), *Aerosol Air Qual. Res*, *13*, 72–82.

Richard, A., et al. (2011), Source apportionment of size and time resolved trace elements and organic aerosols from an urban courtyard site in Switzerland, *Atmos. Chem. Phys.*, *11*(17), 8945–8963, doi:10.5194/acp-11-8945-2011.

Rolph, G. D. (2015), Real-time Environmental Applications and Display sYstem (READY), NOAA Air Resources Laboratory, Silver Spring, Md. [Available at http://ready.arl.noaa.gov.]

Safai, P. D., M. P. Raju, P. S. P. Rao, and G. Pandithurai (2014), Characterization of carbonaceous aerosols over the urban tropical location and a new approach to evaluate their climatic importance, *Atmos. Environ.*, *92*, 493–500, doi:10.1016/j.atmosenv.2014.04.055.

Sahani, M., N. A. Zainon, W. R. Wan Mahiyuddin, M. T. Latif, R. Hod, M. F. Khan, N. M. Tahir, and C.-C. Chan (2014), A case-crossover analysis of forest fire haze events and mortality in Malaysia, *Atmos. Environ.*, *96*, 257–265, doi:10.1016/j.atmosenv.2014.07.043.

Santoso, M., P. K. Hopke, A. Hidayat, and L. Diah Dwiana (2008), Sources identification of the atmospheric aerosol at urban and suburban sites in Indonesia by positive matrix factorization, *Sci. Total Environ.*, *397*(1–3), 229–237, doi:10.1016/j.scitotenv.2008.01.057.

Satterfield, D. (2015), *Southeast Asia Is Burning, and You Can See It from the Moon*, AGU Blogosphere, Washington, D. C.

Schauer, J. J., W. F. Rogge, L. M. Hildemann, M. A. Mazurek, G. R. Cass, and B. R. T. Simoneit (1996), Source apportionment of airborne particulate matter using organic compounds as tracers, *Atmos. Environ.*, *30*(22), 3837–3855, doi:10.1016/1352-2310(96)00085-4.

Seneviratne, M., V. A. Waduge, L. Hadagiripathira, S. Sanjeewani, T. Attanayake, N. Jayaratne, and P. K. Hopke (2011), Characterization and source apportionment of particulate pollution in Colombo, Sri Lanka, *Atmos. Pollut. Res.*, *2*(2), doi:10.5094/APR.2011.026.

Song, C. H., and G. R. Carmichael (1999), The aging process of naturally emitted aerosol (sea-salt and mineral aerosol) during long range transport, *Atmos. Environ.*, *33*(14), 2203–2218, doi:10.1016/S1352-2310(98)00301-X.

Song, Y., S. Xie, Y. Zhang, L. Zeng, L. G. Salmon, and M. Zheng (2006), Source apportionment of $PM_{2.5}$ in Beijing using principal component analysis/absolute principal component scores and UNMIX, *Sci. Total Environ.*, *372*(1), 278–286, doi:10.1016/j.scitotenv.2006.08.041.

Stockwell, C. E., et al. (2016), Field measurements of trace gases and aerosols emitted by peat fires in central Kalimantan, Indonesia, during the 2015 El Niño, *Atmos. Chem. Phys.*, *16*(18), 11,711–11,732, doi:10.5194/acp-16-11711-2016.

Streets, D., K. Yarber, J. H. Woo, and G. Carmichael (2003), Biomass burning in Asia: Annual and seasonal estimates and atmospheric emissions, *Global Biogeochem. Cycles*, *17*(4), 1099, doi:10.1029/2003GB002040.

Tao, J., T. Cheng, R. Zhang, J. Cao, L. Zhu, Q. Wang, L. Luo, and L. Zhang (2013), Chemical composition of $PM_{2.5}$ at an urban site of Chengdu in southwestern China, *Adv. Atmos. Sci.*, *30*(4), 1070–1084, doi:10.1007/s00376-012-2168-7.

Tao, J., J. Gao, L. Zhang, R. Zhang, H. Che, Z. Zhang, Z. Lin, J. Jing, J. Cao, and S. C. Hsu (2014), $PM_{2.5}$ pollution in a megacity of southwest China: Source apportionment and implication, *Atmos. Chem. Phys.*, *14*(16), 8679–8699, doi:10.5194/acp-14-8679-2014.

Technik, G. (2006), *GRIMM Ambient Dust Monitor #365 User Manual*, Grimm Aerosol Technik GmbH, Ainring Germany.

Terzi, E., G. Argyropoulos, A. Bougatioti, N. Mihalopoulos, K. Nikolaou, and C. Samara (2010), Chemical composition and mass closure of ambient PM_{10} at urban sites, *Atmos. Environ.*, *44*(18), 2231–2239, doi:10.1016/j.atmosenv.2010.02.019.

Thurston, G. D., and J. D. Spengler (1985), A quantitative assessment of source contributions to inhalable particulate matter pollution in metropolitan Boston, *Atmos. Environ.*, *19*(1), 9–25, doi:10.1016/0004-6981(85)90132-5.

Turpin, B. J., and H.-J. Lim (2001), Species contributions to $PM_{2.5}$ mass concentrations: Revisiting common assumptions for estimating organic mass, *Aerosol Sci. Technol.*, *35*(1), 602–610.

Turpin, B. J., and J. J. Huntzicker (1991), Secondary formation of organic aerosol in the Los Angeles basin: A descriptive analysis of organic and elemental carbon concentrations, *Atmosph. Environ.*, *25*(2), 207–215, doi:10.1016/0960-1686(91)90291-E.

Turpin, B. J., and J. J. Huntzicker (1995), Identification of secondary organic aerosol episodes and quantitation of primary and secondary organic aerosol concentrations during SCAQS, *Atmos. Environ.*, *29*(23), 3527–3544, doi:10.1016/1352-2310(94)00276-Q.

Vallius, M., N. A. H. Janssen, J. Heinrich, G. Hoek, J. Ruuskanen, J. Cyrys, R. Van Grieken, J. J. de Hartog, W. G. Kreyling, and J. Pekkanen (2005), Sources and elemental composition of ambient $PM_{2.5}$ in three European cities, *Sci. Total Environ.*, *337*(1–3), 147–162, doi:10.1016/j.scitotenv.2004.06.018.

Wahid, N. B. A., M. T. Latif, and S. Suratman (2013), Composition and source apportionment of surfactants in atmospheric aerosols of urban and semi-urban areas in Malaysia, *Chemosphere*, *91*(11), 1508–1516, doi:10.1016/j.chemosphere.2012.12.029.

Wåhlin, P., R. Berkowicz, and F. Palmgren (2006), Characterisation of traffic-generated particulate matter in Copenhagen, *Atmos. Environ.*, *40*(12), 2151–2159, doi:10.1016/j.atmosenv.2005.11.049.

Watson, J. G., and J. C. Chow (2001), Source characterization of major emission sources in the Imperial and Mexicali Valleys along the US/Mexico border, *Sci. Total Environ.*, *276*(1–3), 33–47, doi:10.1016/S0048-9697(01)00770-7.

Watson, J. G., N. F. Robinson, J. C. Chow, R. C. Henry, B. M. Kim, T. G. Pace, E. L. Meyer, and Q. Nguyen (1990), The USEPA/DRI chemical mass balance receptor model, CMB 7.0, *Environ. Software*, *5*(1), 38–49, doi:10.1016/0266-9838(90)90015-X.

Watson, J. G., J. C. Chow, and J. E. Houck (2001), $PM_{2.5}$ chemical source profiles for vehicle exhaust, vegetative burning, geological material, and coal burning in northwestern Colorado during 1995, *Chemosphere*, *43*(8), 1141–1151, doi:10.1016/S0045-6535(00)00171-5.

Weber K., Vogel A., Fischer C., van Haren G., and P. Tobias (2010), Airborne measurements of the Eyjafjallajökull volcanic ash plume over northwestern Germany with a light aircraft and an optical particle counter: First results, Proc. SPIE 7832, Lidar technologies, techniques, and measurements for atmospheric remote sensing VI, pp. 78320P-78320P-15.

WHO (2014), Ambient (outdoor) air quality and health.

Xiaoai G., Grimm H., Pesch M., Keck L., Spielvogel J., Schneider F., and Brunnhuber W. (2010), New methods for real-time measurement of environmental airborne particles, bioinformatics and biomedical engineering (ICBBE), 4th International Conference, pp. 1–4.

Xie, Y.-L., P. K. Hopke, P. Paatero, L. A. Barrie, and S.-M. Li (1999), Locations and preferred pathways of possible sources of Arctic aerosol, *Atmos. Environ.*, *33*(14), 2229–2239, doi:10.1016/S1352-2310(98)00197-6.

Yang, W., S. Zhang, J. Tang, K. Bu, J. Yang, and L. Chang (2013), A MODIS time series data based algorithm for mapping forest fire burned area, *Chin. Geogr. Sci.*, *23*(3), 344–352, doi:10.1007/s11769-013-0597-6.

Yokelson, R. J., R. Susott, D. E. Ward, J. Reardon, and D. W. T. Griffith (1997), Emissions from smoldering combustion of biomass measured by open-path Fourier transform infrared spectroscopy, *J. Geophys. Res.*, *102*, 18,865–18,877, doi:10.1029/97JD00852.

Yu, J. Z., J. Xu, and H. Yang (2002), Charring characteristics of atmospheric organic particulate matter in thermal analysis, *Environ. Sci. Technol.*, *36*(4), 754–761, doi:10.1021/es015540q.

Yu, L., G. Wang, R. Zhang, L. Zhang, Y. Song, B. Wu, X. Li, K. An, and J. Chu (2013), Characterization and source apportionment of $PM_{2.5}$ in an urban environment in Beijing, *Aerosol Air Qual. Res.*, *13*(2), 574–583, doi:10.4209/aaqr.2012.07.0192.

Yuan, Z., A. K. H. Lau, H. Zhang, J. Z. Yu, P. K. K. Louie, and J. C. H. Fung (2006), Identification and spatiotemporal variations of dominant PM_{10} sources over Hong Kong, *Atmos. Environ.*, *40*(10), 1803–1815, doi:10.1016/j.atmosenv.2005.11.030.

Zeng, Y., and P. K. Hopke (1989), A study of the sources of acid precipitation in Ontario, Canada, *Atmos. Environ.*, *23*(7), 1499–1509, doi:10.1016/0004-6981(89)90409-5.

Zhang, Q., et al. (2009), Asian emissions in 2006 for the NASA INTEX-B mission, *Atmos. Chem. Phys.*, *9*(14), 5131–5153, doi:10.5194/acp-9-5131-2009.

Zhang, R., et al. (2013), Chemical characterization and source apportionment of $PM_{2.5}$ in Beijing: Seasonal perspective, *Atmos. Chem. Phys.*, *13*(14), 7053–7074, doi:10.5194/acp-13-7053-2013.

Zhang, X., A. Hecobian, M. Zheng, N. H. Frank, and R. J. Weber (2010), Biomass burning impact on $PM_{2.5}$ over the southeastern US during 2007: Integrating chemically speciated FRM filter measurements, MODIS fire counts and PMF analysis, *Atmos. Chem. Phys.*, *10*(14), 6839–6853, doi:10.5194/acp-10-6839-2010.